SIMULATION OF LIQUID/LIQUID MASS TRANSFER IN GAS STIRRED METALLURGICAL REACTORS

by

M. R. R. I. SHAMSI

DEPARTMENT OF METALLURGICAL ENGINEERING

INDIAN INSTITUTE OF TECHNOLOGY KANPUR

JULY, 1989

SIMULATION OF LIQUID/LIQUID MASS TRANSFER IN GAS STIRRED METALLURGICAL REACTORS

A Thesis Submitted
In Partial Fulfilment of the Requirements
for the Degree of
MASTER OF TECHNOLOGY

by
M. R. R. I. SHAMSI

to the
DEPARTMENT OF METALLURGICAL ENGINEERING
INDIAN INSTITUTE OF TECHNOLOGY KANPUR
JULY, 1989

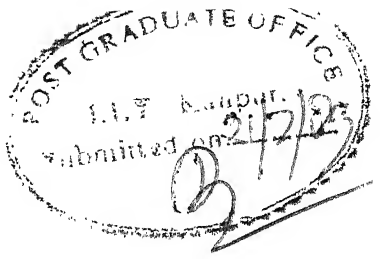

CERTIFICATE

Certified that the work presented in this thesis, "SIMULATION OF LIQUID/LIQUID MASS TRANSFER IN GAS STIRRED METALLURGICAL REACTORS" has been carried out by M.R.R.I.Shamsi under my supervision and that the work has not been submitted elsewhere for a degree.

July, 1989.

Dr. S.C. KORIA
Assistant Professor
Department of Metallurgical Engineerir
Indian Institute of Technology
KANPUR-208016

ACKNOWLEDGEMENTS

As the author, I record at the onset, my great indebtness and deep sense of gratitude to my respected guide Dr. S.C. Koria, for his astute guidance, invaluable suggestion, discussion and freedom to work, keeping a watchful eye on the progress.

I also extend my indebtedness respect and gratitude to Dr. N.K. Batra for his useful advice.

I sincerely acknowledge the help rendered to me by Mr. Sharma of Chemical Metallurgy, Mr. Mangole of Chemical Metallurgy Lab,, Mr. Chaurasia of Analytical Lab., Mr.P.R.Singh of Glass Blowing Lab.

I am grateful to my friends Mr. H.N. Azari, Mr. Anil Kumar, Mr. Pawan Dhameja, Mr. Sarbjit Singh, Miss Uma Devi, Miss Sohini Pal, Mr. N. Kapuri, Mr. R.R.M. Rai for their help.

A special word of appreciation to Mr. U.S. Mishra for his excellent typing.

I am also grateful to those who have directly or indirectly given aid to perform this project.

-M.R.R.I. Shamsi

CONTENTS

NOMENCLATURE

A	Interfacial area
C_e	Equilibrium concentration of benzoic acid
C_o	Initial concentration of benzoic acid
C_t	Concentration at time t of benzoic acid
d	Diameter of disperse particle
d_n	Diameter of nozzle
K_b	Rate constant in bottom injection
K_t	Rate constant in top injection
K	Rate constant
L	Volumetric mass transfer coefficient
m, n	Exponent
$\dot{V}_g$	Gas flow rate
t	Time
T_g	Temperature of gas
T_L	Temperature of liquid
V_L	Volume of liquid
U	Velocity of droplet
U_P	Plume velocity
V_w	Volume of water
β_m	Mass transfer coefficient
β	Depth of submergence of lance
M_T	Mass of benzoic acid in water
$\dot{m}_T$	Mass flux of benzoic acid in the phase boundary
ϕ	Volume fraction of slag

D	Bath diameter
D_f	Diffusion coefficient of benzoic acid in water
μ	Viscosity of water
ρ_L	Density of water
Sc	Schimid number
P_2	Atmospheric pressure
$\dot{\varepsilon}$	Mixing energy
g	Acceleration due to gravity
H	Bath height
α, a	Constant
Re	Reynold number
Sh	Sherwood number
N	Number of nozzle
d_t	Diameter of tuyers
N_{Fr}	Froud No. based on superficial gas velocity
N'_{Fr}	Froud No. based on plume gas velocity
ν	Kinematic viscosity
U_b	Plume velocity in bottom injection
U_t	Plume velocity in top injection.

CHAPTER - 1

INTRODUCTION

1.1 GENERAL

The growth in scope and extent of ladle refining technology has been one of the most significant features of steelmaking developments in recent years. The main reasons for this are as follows[1]:

1. Productivity and costs: By transferring the functions of temperatures and composition adjustment to ladle treatment, the primary furnace can be operated more efficiently as a melting and decarburizing unit. Alloy yields can be improved.

2. Continuous Casting: The use of continuous casting is increasing rapidly. The process requires tight temperature control. Inclusion removal can be a vital factor in ensuring good teeming control.

3. Product Development: Requirements by the customer for tighter composition control, very low sulphur content or very clean steels are becoming increasingly common.

The present investigation concerns with the physical modelling of liquid/liquid mass transfer without chemical reaction in gas stirred ladles.

1.2 EQUATION OF TRANSPORT AND BALANCE FOR MASS TRANSFER

Because of conservation of mass the change in concentration of solute in the aqueous solution is

$$\frac{dC_t}{dt} = - \frac{\dot{m}_T}{V_w} \tag{1.1}$$

$$C_t = \frac{m_T}{V_w} \tag{1.2}$$

By linear expression the irreversible mass flux is mostly combined with the corresponding thermodynamic forces.

$$\dot{m}_T = L\,(C_t - C_e) \tag{1.3}$$

$$L = \beta_m \cdot A \tag{1.4}$$

Using equations (1.3) and (1.1) and integrating with the initial condition $C_t\ (t = 0) = C_o$ yields

$$C_t = C_e + (C_o - C_e) \cdot \exp\left(- \frac{L \cdot t}{V_w}\right) \tag{1.5}$$

By equating (1.5),

$$L = \frac{V_w}{t} \cdot \ln \frac{(C_o - C_e)}{(C_t - C_e)} \tag{1.6}$$

$$\ln \frac{(C_t - C_e)}{(C_o - C_e)} = - \frac{L}{V_w} \cdot t$$

so,

$$\ln\left(\frac{C_t - C_e}{C_o - C_e}\right) = -Kt \qquad (1.7)$$

$$K = \frac{\beta_m . A}{V_w} = \text{rate constant} \qquad (1.8)$$

Equation (1.7) can be used to determine the rate constant (K) at known equilibrium concentration C_e by measuring the concentration C_t in dependence of the time. K value signifies how well or bad phases are stirred. In the case of a gas stirred system it is difficult to measure interface area. So volumetric mass transfer ($\beta_m . A$) and K is reported to know the comparative extent of mass transfer.

1.3 LITERATURE SURVEY

Shiego Asai et. al studied the connection between mass transfer rate and the behaviour of liquid-liquid interface in the model experiment[2].

They found that at critical point where a part of slag layer is entrapped in metal layer by vigorous agitation, there area abrupt change in the dependence of gas flow rate on the volumetric mass transfer coefficient (L). Volumetric mass transfer coefficient has been defined in equation (1.4).

Quying et. al[3] and Sakare et. al[4] studied mixing and mass transfer in model ladle. They found that rate of slag-metal mass transfer is increased with stirring energy.

The stirring energy was calculated by following equation[5];

$$\dot{\varepsilon} = \frac{6.18 . V_g . T_L}{V_L \rho_L} \left[\ln \left(1 + \frac{\rho_1 g H}{P_2}\right) + \left(1 - \frac{T_g}{T_L}\right) \right] \quad (1.9)$$

$\dot{\varepsilon}$ = mixing energy watt/ton

V_g = gas flow rate Nm^3/min

T_L = temperature of liquid ^oK

V_L = vol. of bath (m^3)

ρ_L = density of liquid (ton/m^3)

g = acceleration due to gravity (m/sec^2)

H = bath height (m)

P_2 = atmospheric pressure ($kg\ m^{-1}\ sec^{-2}$)

ρ_1 = 1000 kg/m^3

T_g = temperature of gas (^oK)

They also concluded that smaller energy is sufficient for homogenisation by Ar stirring but a large energy supply is necessary for slag metal in the ladle. QU YING et al[3] concluded that ecentric placing of lance is beneficial to mixing but it is disadvantageous to slag metal mass transfer. The experimental results of Seon-Lyo et al[6] support the above statement.

Masahiro et al[7] studied transfer of Si from molten Cu to FeO slag. They also studied the influence of bath height, slag height on the transfer of Si from Cu to FeO.

They found that the apparent mass transfer coefficient increased with increasing gas injection rate but the dependence of apparent mass transfer coefficient on gas flow rate changes at transition gas flow rate. They observed three regions in which apparent mass transfer coefficient changes differentially with gas flow rate.

K. Ogawa et al[8] has studied slag-metal mass transfer coefficient in gas stirring and induction stirring in water model and plant scale experiments. Metal phase mass transfer coefficient in model and plant scale were correlated to parameter $\dot{\varepsilon}\ \dot{V}_g^{-2/3}$.

The metal phase mass transfer coefficient for gas bubbling was found to be larger than for induction stirring.

1.4 OBJECTIVE OF PRESENT INVESTIGATION

The present investigation is a cold model study of liquid/liquid mass transfer due to gas injection in metallurgical reactor. Benzoic acid is used as a transferring entity from water to oil.

In the experimental programme, photographic investigations are made to illustrate qualitatively the influence of gas injection parameters on the behaviour of the phases. Detailed measurements are then made on the transfer of benzoic acid from water phase to oil phase over a wide range of gas flow rate and injection parameters. The gas is injected

through the centre of the base of the vessel and from top by submerging a lance into the water bath. Influence of the volume of the model slag on the rate of benzoic acid transfer is also studied. Some experiments are also performed by injecting gas through the side of the vessel. For these experiments separate vessel is fabricated. In these experiments the influence of gas injection rate on mass transfer could only be studied.

Several experiments are performed by injecting model slag into the bath.

CHAPTER 2

SIMULATION CRITERIA

The present investigation aims at to study the mass transfer controlled by metal side.

Experimental results from model can be confidently applied to the actual process only if the condition of similarity are maintained. For system with uniform temperature distribution, these condition will be met if the ratios of the various lengths, velocities and forces between corresponding points in each system are fixed. Therefore, the model, as far as possible must have the same shape as the prototype, the fluid flow streamlines must be geometrically similar, and the values of the dimensionless groups which represent force ratios must have the same value in each system.

2.1 GEOMETRICAL SIMILARITY

For geometrical similarity following consideration are applied:

$$\text{Aspect ratio } (\phi) = \frac{H}{D} \qquad (2.1)$$

Aspect ratio signifies shallow or deep bath and assimilation of energy supply to the bath.

In industrial ladle it is 0.95 to 1.2[9]. In our present investigation it taken to $\frac{19}{20} = 0.95$.

In selecting diameter of the injection nozzle no satisfactory criteria could be determined from the literature[10-18]. In the absence of a suitable criterion diameter of the gas injection nozzle is arbitrarily fixed to 1 mm in the present investigation. This arbitratory selection of diameter is not considered to influence the objective of the investigation as long as gas injection mode (Bubbling or jetting) in the cold model system is kept similar to industrial system (Hot metal/gas). In this connection it may be noted that the flow rate used for stirring in treatment of steel in ladles, the fluid dynamics in the ladle are governed by a buoyancy plume rather than a jet model.

2.2 DYNAMICAL SIMILARITY

Dynamic similarity requires that the forces acting at corresponding time and on corresponding locations in the model and in the prototype bear a fixed ratio. In the literature on simulation of gas stirring in ladle, modified Froude number and the Reynold number are normally used to quantify the magnitude of the forces.

In the literature few definition of the Froude number are available, one based on the superficial gas injection velocity and the other on the plume velocity,

$$N_{Fr} = \frac{\rho_g \; u^2}{\rho_l \; g \; H} \qquad (2.2)$$

This no compares the gas dynamic pressure at the nozzle exit with the hydrostatic pressure at the same point. Its similarity ensures the identical behaviour of gas at the exit of a nozzle submerged in the model liquid and steel melt.

Value of Froude number in industrial practice is generally varied from 0.96 to 1.3[9].

In our work it is varied from 0.042 to 24.04.

Froude number based on plume velocity is given by

$$N'_{Fr} = \frac{U_p^2}{g \times 0.37 \times H} \qquad (2.3)$$

where

$$U_p = \frac{K' \ \beta^{1/3} \times H^{1/4} \times \dot{V}_g^{1/3}}{R^{1/3}} \qquad (2.4)$$

g = 9.81 m /sec^2, H in m, R in m, $\dot{V}$ in m^3/sec, U_p m/sec.

β = depth of the lance = Depth of lance/Bath height

For typical industrial practice[6-19]

H = 3 meter

R = 1.5 meter

$\dot{V}_g$ is varied from 425 Nl/min to 800NL/min.

Inserting these values into equation (2.3) and equation (2.4), we obtain N'_{Fr} for bottom injection = $2.13 \dot{V}_g^{2/3}$. (2.5)

Putting the value of $\dot{V}_g$ in equation (2.5).

We get N'_{Fr} from 0.078 to 0.119

In our model study N'_{Fr} is varied from 0.0217 to 0.18. For top injection putting β = 0.5, we get

$$N'_{Fr} = 1.34 \times \dot{V}_g^{2/3} \qquad (2.6)$$

Putting the value of $\dot{V}_g$ we get N'_{Fr} from 0.049 to 0.07. In our model study it is varied from 0.014 to 0.114.

CHAPTER 3

EXPERIMENTAL

The experimental programme of the present investigation consists of two parts: photographic work and quantitative measurement.

3.1 EXPERIMENTAL SET-UP

Figure 3.1 show the experimental set-up used in this study. The diameter of the vessel is 20 cm and height is 25 cm. One end of the vessel is closed with a bottom plate using a rubber gasket. In this plate a hole is drilled in the centre to insert the nozzle for gas injection. Air is used to stirr the bath. It is introduced through the bottom of the vessel by a 1 mm diameter nozzle and varied from 0.5 to 12 Nl/min. Several experiments are also performed in which gas is introduced through the top of the vessel by a lance submerged in the bath. All the experiments are performed at the value of $\beta = 0.5$. This value of β is very commonly employed in treatment of steel in ladles by injecting gas through a top lance. The lance diameter is 1 mm. It is fabricated by glass.

Figure 3.2 shows the design of a model slag injector and setup used in this study. It is constructed from a pipe

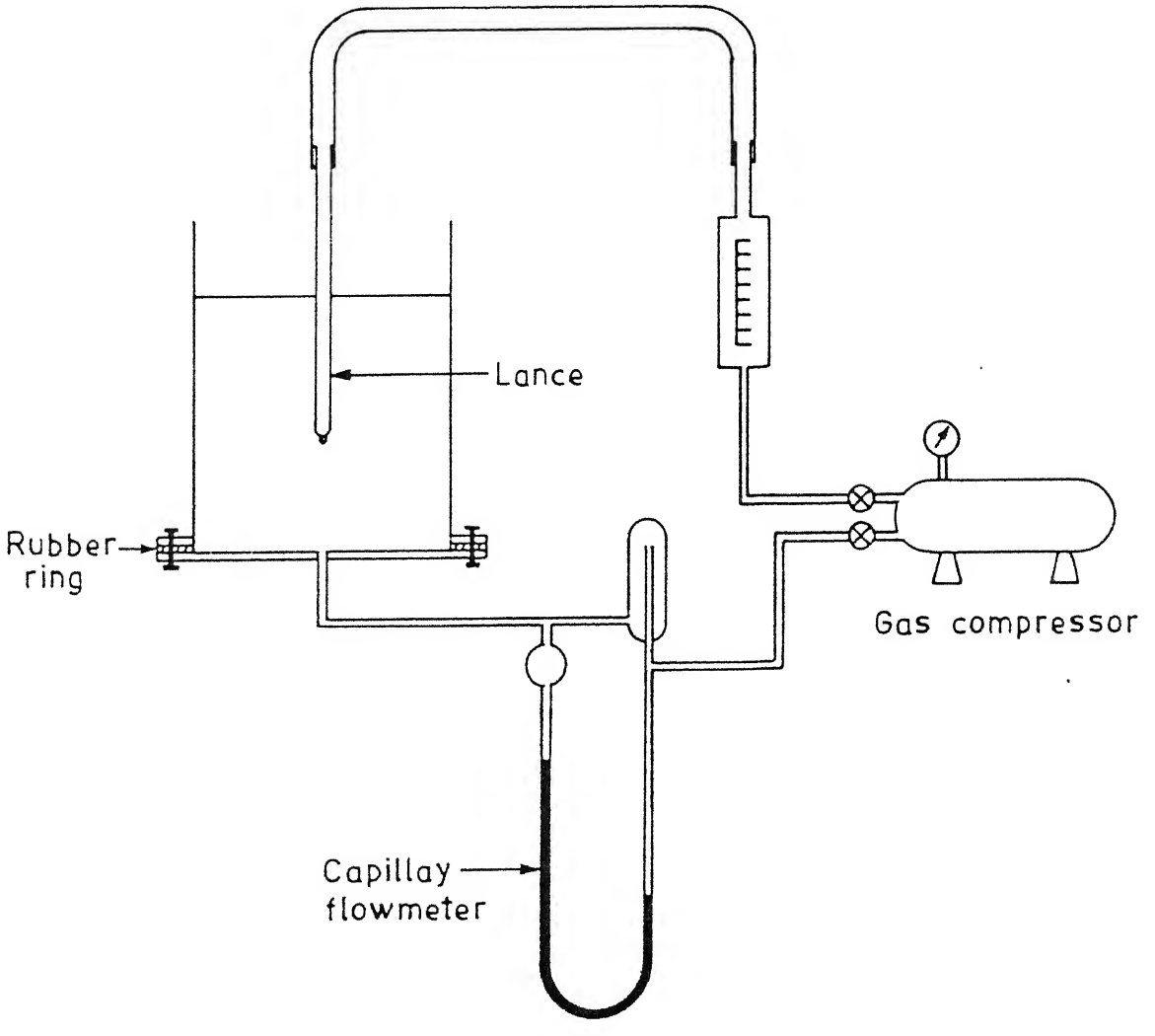

Fig. 3.1 : Schematic representation of experimental set-up for bottom and top injection.

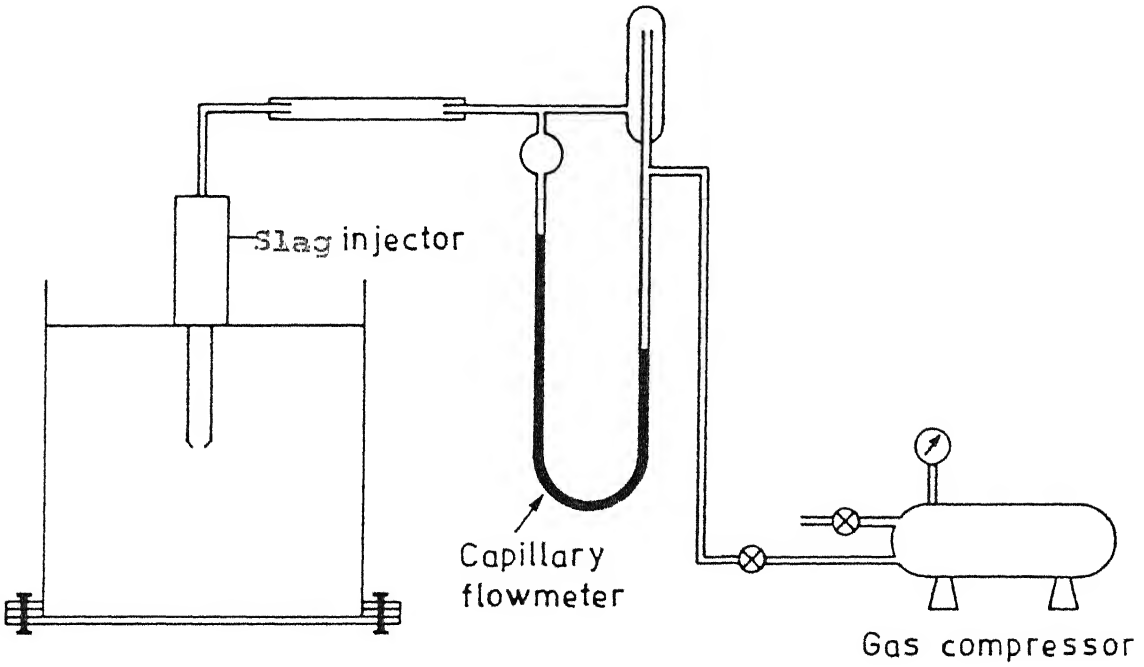

Fig. 3.2: Schematic representation of experimental set-up for Slag injection.

of inner diameter 5.6 cm and outer diameter 6.0 cm and length 34 cm. Both the open end of the pipe are closed. One end of the pipe is used to inject the gas and also to fill the injector with the model slag. The other end of the pipe is provided with a hole in which different diameter nozzles can be inserted as per the need of the investigation. The open end of the nozzle is closed by a cap in order to avoid the flow of model slag during filling in the pipe.

Some experiment have been done by side injection also. For these experiment semicylindrical vessel has been used as shown in Fig. 3.3. This has the flat face 40 cm x 40 cm and Y joint nozzle of 2 mm diameter is used for gas injection. 12 litre aqueous solution is used for gas injection.

3.2 CALIBRATION OF CAPILLARY FLOW METER

This has been done by means of a wet-test flow meter. Two capillary flow meters has been used for the present study. One is for lower range of flow rate - 1 NL/mm to 2.5 NL/min, another is for higher range of flow rate - 3 NL/min to 12 NL/min. Their calibration curves have been given in Figures 3.4 and 3.5.

3.3 CHOICE OF MASS TRANSFER SYSTEM

A low temperature mass transfer system such as distribution of a solute between two immiscible liquid phases is selected for the present study. Such a system

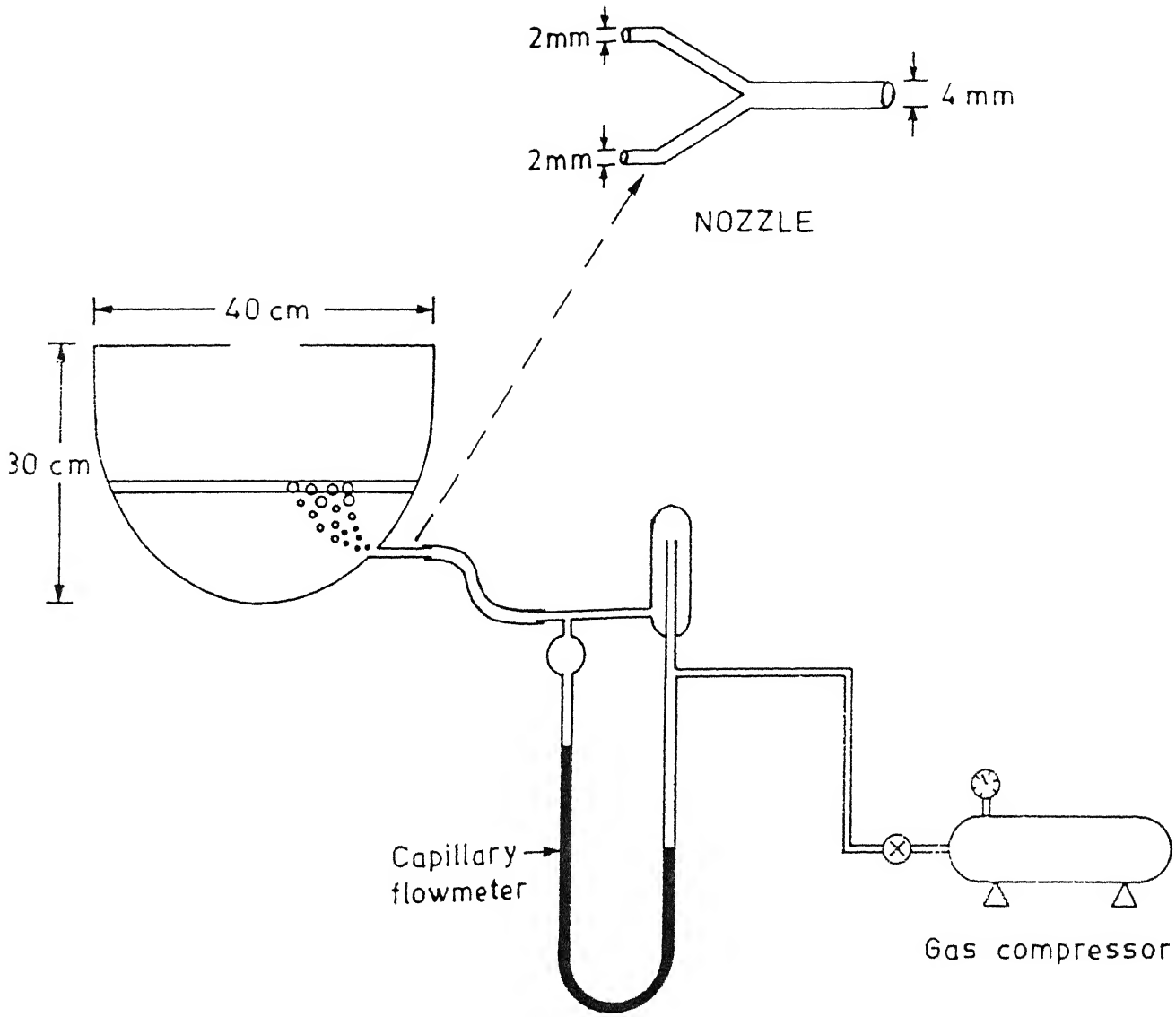

Fig. 3.3 : Schematic representation of experimental set-up for side injection.

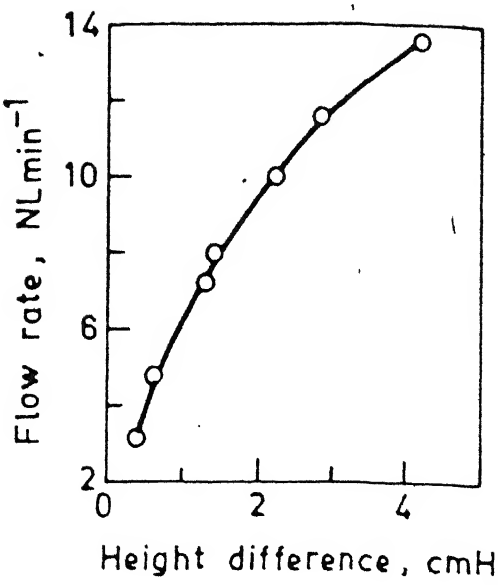

Fig.3.4 Calibration curve for capillary flow meter for higher range of gas flow rate

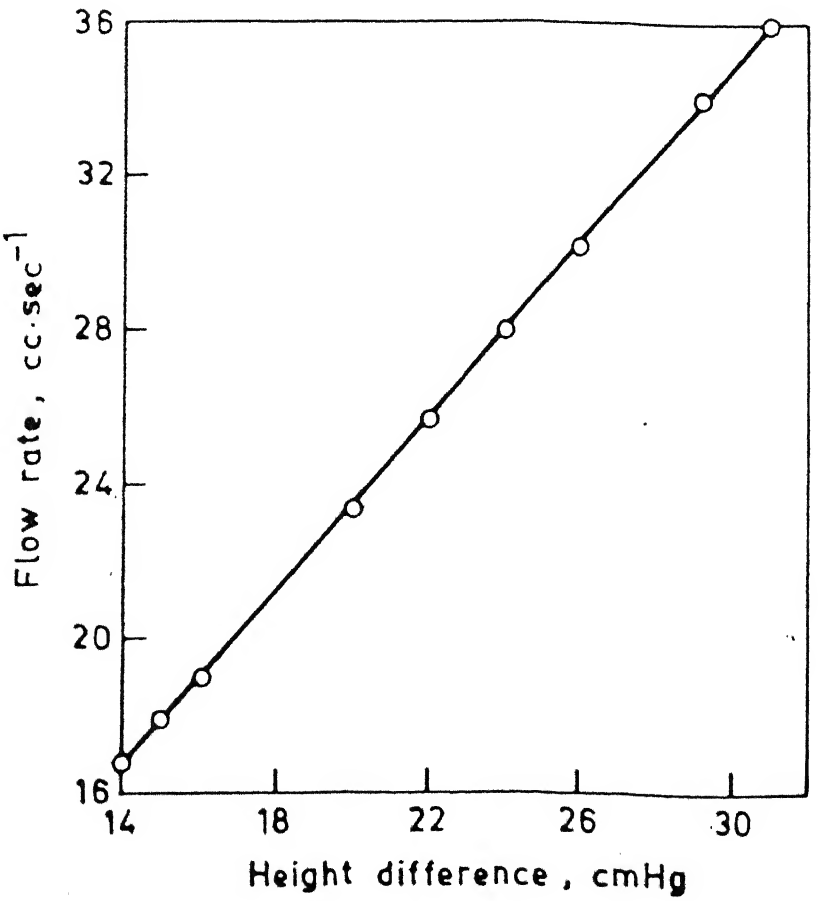

Fig.3.5 Calibration curve for capillary flow meter for lower range of gas flow rate.

is easier to handle in laboratory than molten metal/slag. The two liquids used are water (Phase I) and 1:1 mixture of heavy paraffin oil and toluene (Phase II). For quantitative measurement benzoic acid is used as the transferring entity from Phase I to Phase II. For photographic investigation iodine is added in oil phase to colour it. This is done to increase the contrast between water and oil phase. With this technique it is possible to isolate the model slag clearly on the photographs.

3.4 PREPARATION OF LIQUID

Phase I is an aqueous solution of benzoic acid and is prepared in bulk so that for each experiment the same strength of the aqueous phase is available. A saturated solution of benzoic acid (2.32 gm/litre) is made by dissolving it in distilled water and then filtering it to obtain a clear solution. The strength of the benzoic acid solution is determined by usual titration method. It is made constant by addition of fixed. Calculated amount of distilled water. Phase II is prepared by mixing equal volumes of heavy liquid paraffin and toluene. This mixture is stirred well before starting the experiment.

For photographic investigation iodine is added in oil phase to colour it.

3.5 SOLUTION FOR TITRATION

The concentration of benzoic acid solution in the main experiment is determined by titration. For this purpose oxalic acid and KOH solutions are prepared.

A standard solution of (0.1N) oxalic acid is prepared by dissolving exactly 1.575 gm of hydrated oxalic acid ($H_2C_2O_4 \cdot H_2O$) in distilled water taken in a 250 ml. Standard flask.

Equivalent wt. of oxalic acid = 63

$\therefore$ Strength of the solution $= \frac{1.575}{63} \times \frac{1000}{250}$

$= 0.1N$

A standard solution of KOH can not be prepared by direct weighing. So an approximately N/10 solution of KOH is prepared by dissolving about 5.6 gm of KOH in one litre of distilled water.

Now 25 ml of the standard oxalic acid is pipetted out into a conical flask and titrated against this KOH solution using phenolphthalein as indicator. The end point is the first appearance of a permanent pink colour. The experiment is repeated till consecutive cocordant values are obtained.

25 ml of oxalic acid = 25.5 ml of KOH

Normality of KOH $= \frac{0.1 \times 25}{25.5} = 0.09804$

This solution of KOH is diluted 5 times and used for titrating benzoic acid solution.

3.6 EXPERIMENTAL PROCEDURE

3.6.1 Photographic Investigation

For photographic investigation, the experimental procedure is as follows: 1.3 litre water has been taken in the glass vessel of diameter 13 cm and height 18 cm. 0.21 litre of oil mixture has been coloured by adding iodine solution, then it has been poured carefully along the side of the vessel. Gas has been injected from top and bottom independently at different flow rates. Photographs of two phase solution has been taken at different gas flow rate.

The camera used is Canon AR1 SCR with shutter speed $\frac{1}{125}$ and aperture 5.6. A Fuji (400 ASA) colour film is used and the source of light is 2x1000W tungsten filament.

3.6.2 Quantitative Measurement

A definite amount of gas is injected in the plexiglass vessel by adjusting the gas tap. Then 5.5 litre of the aqueous solution of the benzoic acid is taken in the vessel and the oil mixture is poured carefully along the sides of the vessel and a stop-watch is simultaneously started (time of pouring of paraffin oil is less than 5 sec). Temperature of the liquid is measured by a thermometer. After 1 minutes 25 ml of liquid I is pipetted out carefully

and titrated against standard KOH solution using phenolphthalein as indicator. The first appearance of a permanent pink colour represents the end point of the reaction. All the sample is taken from the same point. The above titration method is repeated for 3,5,10,15,20,25 minutes. The reproductibility of the results are check by repeating a few experiments and the error in measurement is found to be $\pm$ 4%.

In this way experiments are performed and for each experiment fresh liquids of same composition is used.

For the slag injection first nozzle is closed with the help of a cap. The e: ment with the injection of model slag is carried out in the set-up as shown in Fig. 3.3. For this purpose 5.5 litre water solution is taken. The injector with the model slag is positioned at the top of the vessel. Now a nominal pressure is applied so that all the slag should come out from the injector. The injector is submerged into a model bath at the desired depth. The cap is opened and simultaneously the stop watch is started. The sample were taken at different time.

With side injection the required rate of gas flow is adjusted then 12 litre of water is poured in the vessel. 1.2 litre of model slag is added gently on the water surface and simultaneously the stop watch is started. The duration of the experiment is 45 minutes and sample are taken at the interval of 5 minutes.

3.7 SELECTION OF EXPERIMENTAL VARIABLES

The following variables are studied in different types of experiment.

3.7.1 Bottom Injection

Following variables are studied in bottom injection in order to know their influence on mass transfer.

(a) Gas Flow Rate:

Gas flow rate is varied from 0.5 NL/min to 12 NL/min . This large range of gas flow rate is taken for better understanding of two phase behaviour.

(b) Volume of Slag:

500 ml,875 ml and 1100 ml slag is taken.

3.7.2 Top Injection

Following variable is studied:

(a) Gas Flow Rate:

The gas flow rate is varied from 0.5 NL/min to 12 NL/min .

(b) Volume of Slag:

500 ml and 875 ml slag is taken.

3.7.3 Slag Injection

Following variable is studied in this:

(a) Nozzle Diameter:

The nozzle diameter is 0.1 cm and 0.2 cm.

(b) Volume of Slag:

Volume of slag is 275 ml and 550 ml.

(c) Depth of Submergence of Lance Injector:

The depth submergence of slag injector (in terms of bath height) is 0.5 and 0.95.

3.7.4 Side Injection

The gas flow rate is varied from 9 NL/min to 40 NL/min .

CHAPTER 4

RESULTS AND DISCUSSION

In this chapter the experimental results on photographic investigation and quantitative measurements and their discussion are presented.

4.1 PHOTOGRAPHIC RESULTS AND GENERAL OBSERVATIONS

Photographic study is done to know qualitative the behaviour of the phases (water and oil) due to injection of gas. Gas is injected fro: top and bottom independently. Paraffin oil is coloured intense voilet in order to improve the visibility of the behaviour of slag phase. In all the photographs the coloured region is the paraffin oil (model slag) and colourless region is water (model bath).

Photographs 1-3 show the behaviour of the phases due to top injection of gas through a top lance submerged in the water bath to half the bath height while photograph 4-6 shows due to bottom injection of gas.

Top lance has the nozzle diameter 1 mm. Now gas is injected through the top lance for very low gas flow rate ($\dot{V}_g$ = 1 NL/min, N_{Fr} = 0.242, N'_{Fr} = 0.055). Wavy interface is observed. No oil droplet formation is observed (see photograph 1). Visual observation has indicated that

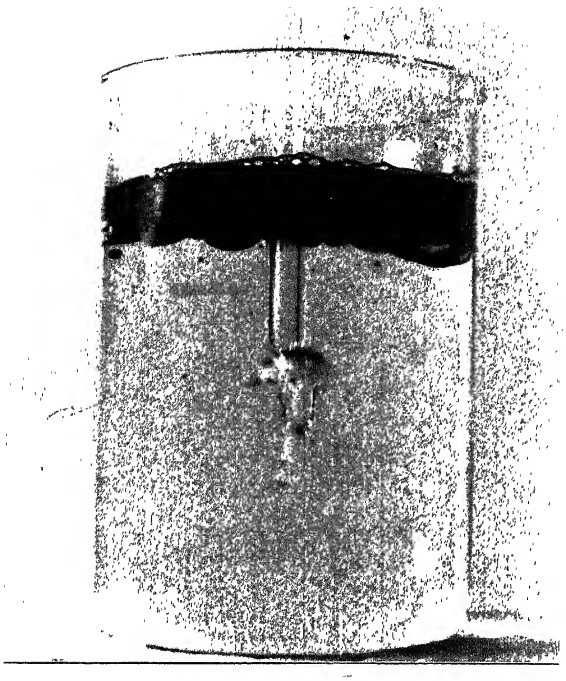

Fig. 1 $\dot{V}_g$ = 1 NL/min

g. 2 $\dot{V}_g$ = 3 NL/min

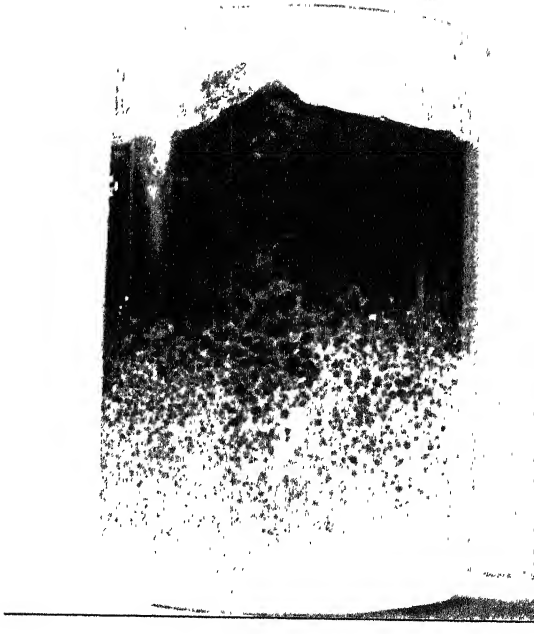

Fig. 3 $\dot{V}_g$ = 9 NL/min

otographs showing the behaviour of two immiscible phases (water and
1 phase coloured by iodine) under the action of top injection.

Fig. 4 $\dot{V}_g$ = 1 NL/min.

Fig. 5 $\dot{V}_g$ = 3 NL/min

Fig. 6 $\dot{V}_g$ = 6 NL/min

Photographs showing the behaviour of two immiscible phases (water and oil phase coloured by iodine under the action of bottom gas injection.

further increase in gas flow rate resulted into the formation of oil filaments which then break-up and formation of drops takes place.

Photograph 2 show the behaviour of two phases at gas flow rate $\dot{V}_g$ = 3 NL/min, N_{Fr} = 1.64, N'_{Fr} = 0.115. Droplets are formed and they entrain into the bath.

Photograph 3 show the behaviour of two phases at gas flow rate $\dot{V}_g$ = 9 NL/min, N_{Fr} = 4.92, N'_{Fr} = 0.871.

It can be seen that the major portion of the slag volume in the form of droplets entrained into the model bath. Further the depth of entrainment of the cloud of oil droplets into model bath is significantly higher than that for condition of photograph 2.

The amount of entrainment of these droplets is found to be dependent on the intensity of gas injection. It may be noted in the photograph that the droplet of different sizes are produced. Visual observation has shown that the diameter of these droplets depend on gas injection rate. Higher gas injection rate has produced more fine than that of low gas injection rate. The diameter of these droplet are estimated to lie in between 1-6 mm; the upper limit depends on intensity of gas injection rate.

For bottom injection (see photographs 4-6) the behaviour of oil phase is found to be qualitatively similar

to that presented for top gas injection (Photograph 1-3). However the observations differed quantitatively with respect to the value of gas injection rate. For top lancing higher gas injection rates were required than for bottom injection in order to produce an approximately similar behaviour. For example compare photograph 3 and 6. In both these photographs the depth of entrainment of the cloud of oil droplets is nearly same (although for bottom injection it is some what higher). But for top injection 9 NL/min gas injection rate is required whereas for bottom injection it was 6 NL/min.

An intrepretation of the results of the photogfaphic investigation for the purpose of mass transfer studies will suggest that mass transfer rate should be function of gas injection rate and method of supply of gas into the bath. Qualitatively the mass transfer should be higher for bottom injection than for top injection (for similar gas injection rate, slag volume).

Similarly there should also exist the different regimes dependence of mass transfer on gas injection rate. This photographic and visual observation have encouraged to do quantitative experiment. The experimental results on quantitative observation (See Section 4.2 and Chapter 4) confirms the above derived information from the photograph.

4.2 QUANTITATIVE MEASUREMENT

All the results of measurement of the change in concentration of benzoic acid with respect to time for injection of slag and without slag injection are reported in Table 4.1 . In the following, the experimental results are presented according to variable affecting them.

4.2.1 Top Submerged Injection of Gas

In these experiments air is injected from top by submerging the lance into the model bath. The depth of submergence (depth of lance submergence/model bath height) is 0.5 for all the experiments reported in this section.

4.2.1.1 Influence of Gas Injection Rate

Figure 4.1 shows the variation of fraction concentration (C_t/C_o) of benzoic acid in water resulting due to its transfer into the 550 ml oil (volume fraction of model slag = $\phi = \frac{\text{Volume of model slag}}{\text{Volume of model bath}} = 0.1$) vs. time for various gas injection rate and Fig. 4.2 for 875 ml of oil ($\phi = 0.5$).

The experimental set-up is shown in figures. It can be seen in the figures that as gas flow rate increases C_t/C_o decreases which implies increased transfer of benzoic acid to oil.

For example consider the value of C_t/C_o at 15 minutes for various gas flow rate and $\phi = 0.1$. This value is 0.946

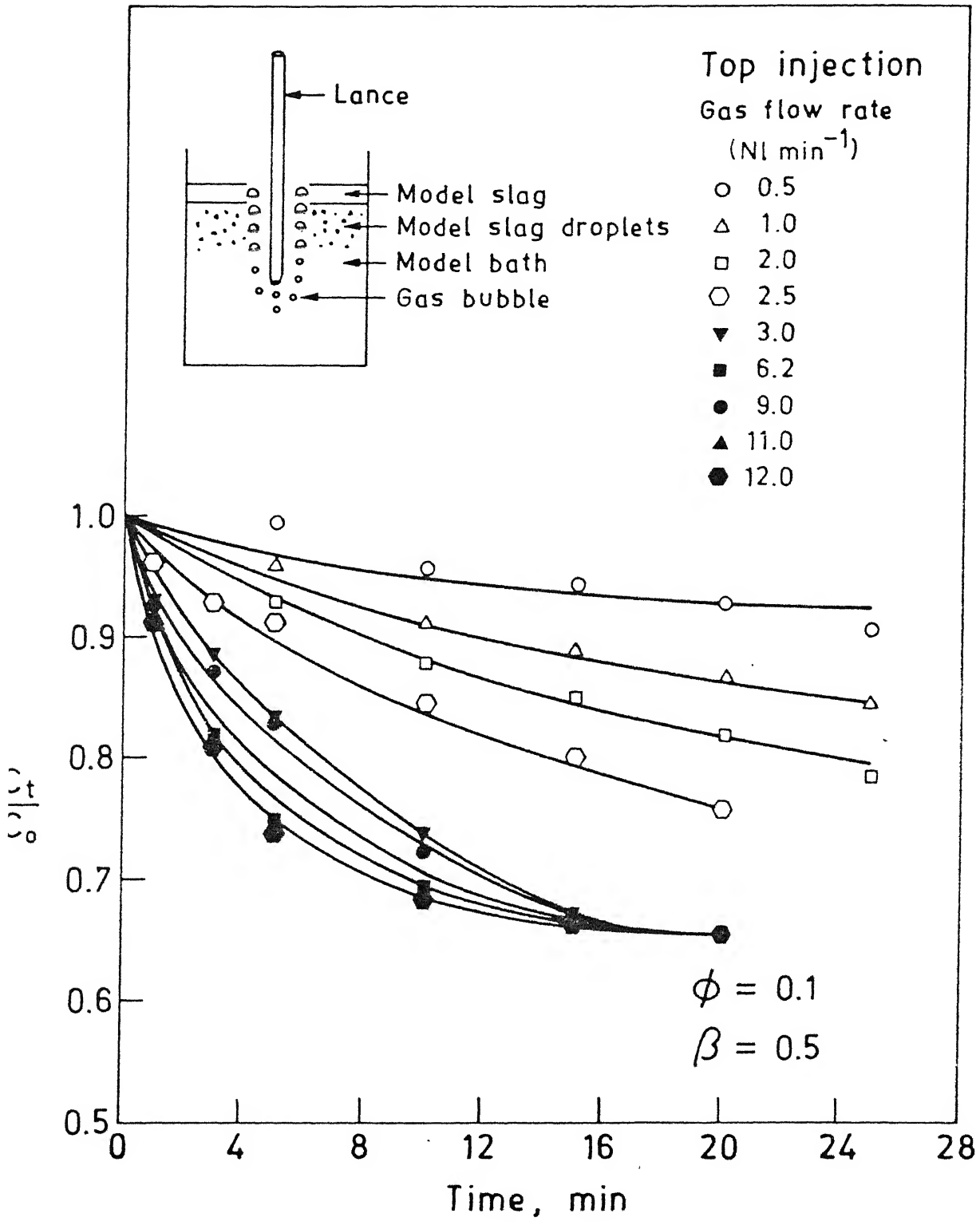

Fig.4.1 : Fractional change of concentration of benzoic acid in water vs. time during top submergence injection (β = 0.5) at various gas flow rate and for volume fraction of gas slag = 0.1.

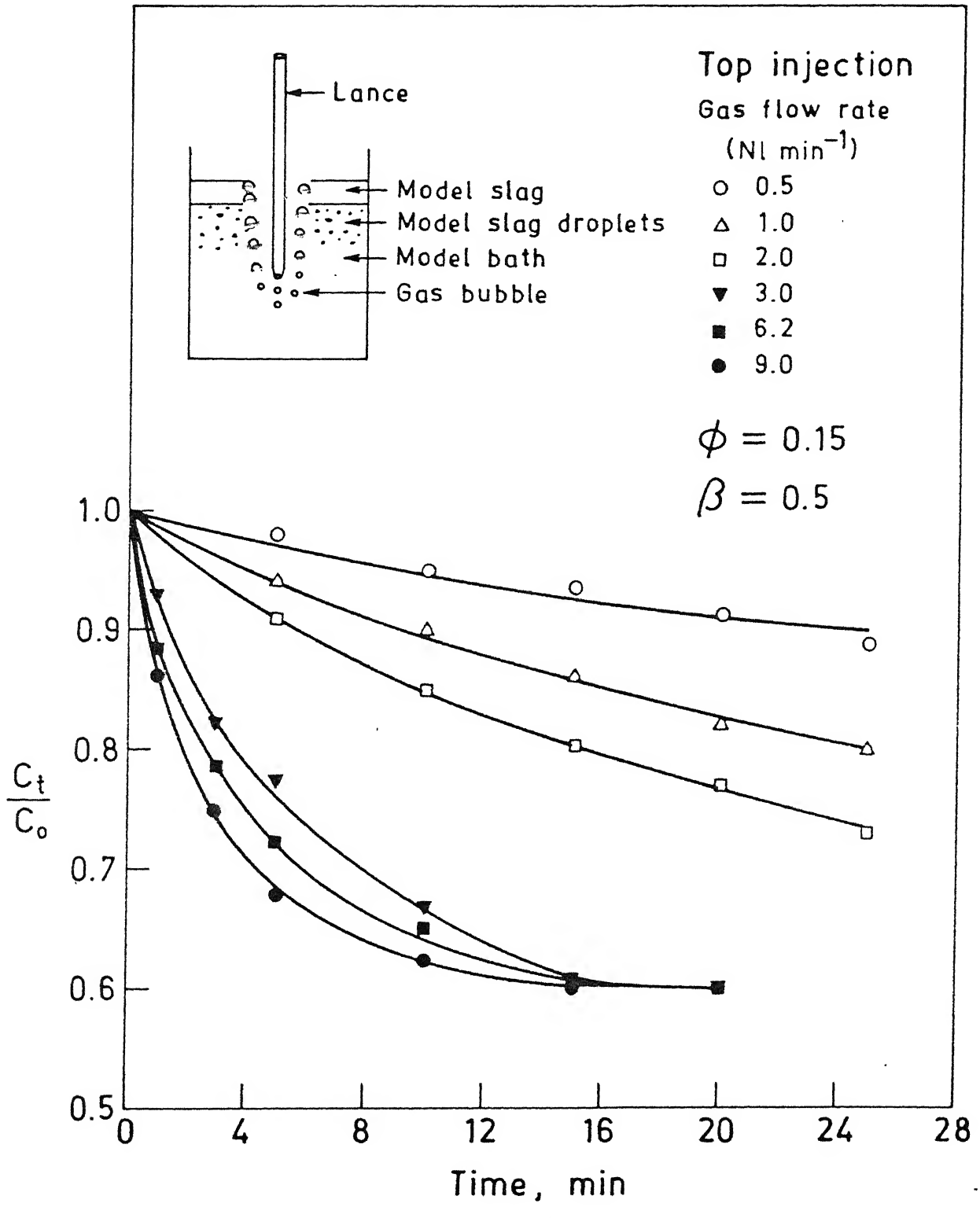

Fig. 4.2 : Fractional change of concentration of benzoic and acid in water vs. time during top submergence injection (β = 0.5) at various gas flow rate and for volume fraction of slag 0.15.

at 0.5 NL/min, 0.89 at 2 NL/min, 0.85 at 2.5 NL/min, 0.677 at 3 NL/min, 0.677 at 6.2 NL/min, 0.677 at 9 NL/min, 0.677 at 11 NL/min and 0.677 at 12 NL/min.

It can also be seen in both figures that for high gas flow rate 2 NL/min after some time there is no more transfer of benzoic acid from water to oil about equilibrium value.

To further check that whether there is more transfer of benzoic acid, sample has been taken after one hour, two hour and four hour after the experiment. No more transfer of benzoic acid from water has been found, so this last value has been taken as equilibrium.

Following are the value of equilibrium constant at differen volume fraction of slag:

$$\emptyset = 0.1 \quad C_e = 1.554$$
$$\emptyset = 0.15 \quad C_e = 1.38$$
$$\emptyset = 0.2 \quad C_e = 1.26$$

4.2.1.2 Influence of Volume Fraction of Slag

Figure 4.3 compares the influence of slag volume on the change of fractional concentration of benaoic acid in water with respect to time for different gas flow rate, i.e. 1 NL/min^{-1} and 3 NL/min^{-1}.

It can be seen in the figure that increase in slag volume fraction of slag decreases the ratio C_t/C_o for sll times and at all gas injection rate. For example for 550 ml

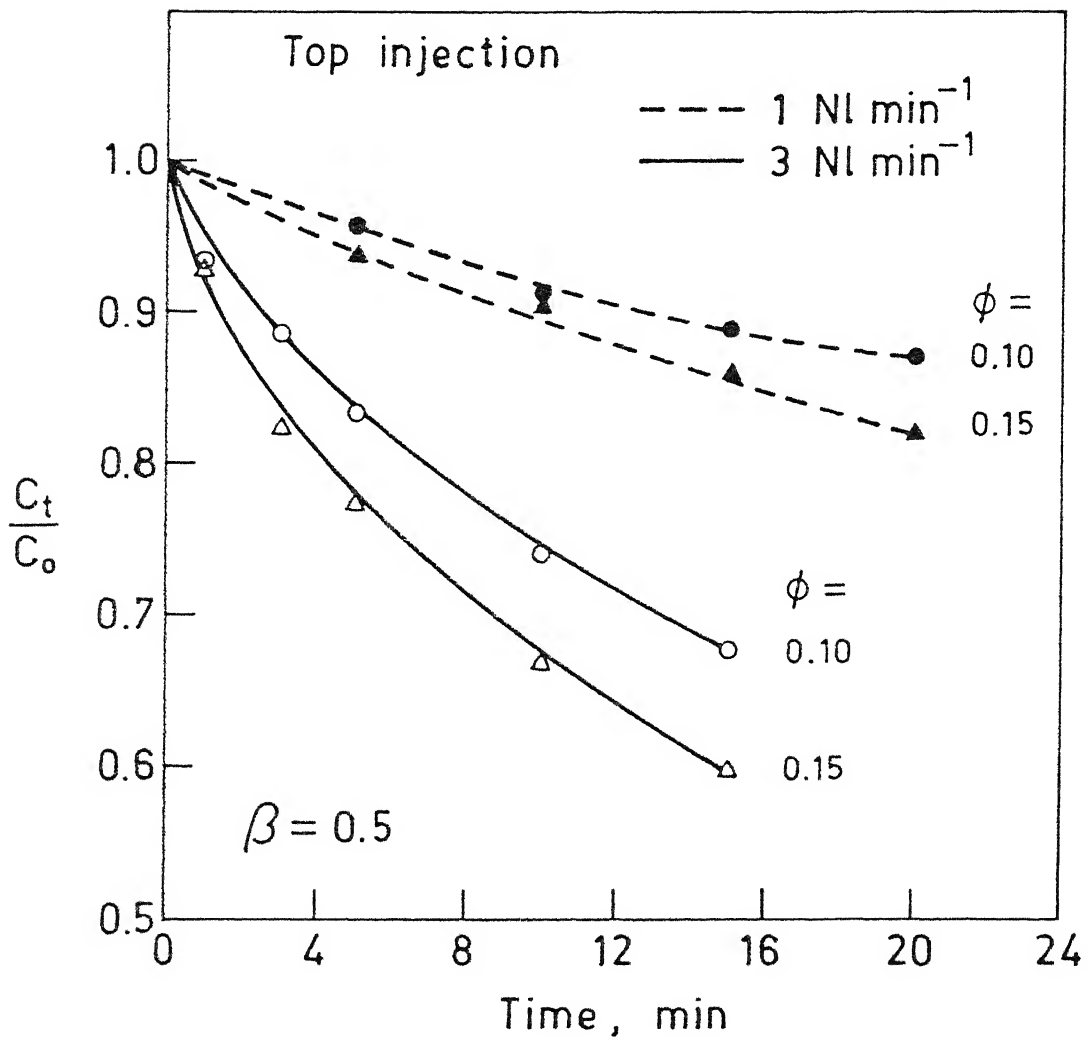

Fig. 4.3 : Fractional change of concentration of benzoic acid in water vs. time during top submergence lance for 0.1 and 0.15 volume fraction of slag at two gas flow rate (1 and 3 NL/min).

slag volume (ϕ = 0.1) and 1 NL/min gas injection C_t/C_o is 0.868 after 20 minutes whereas for 875 ml slag volume (ϕ = 0.15) and at same gas injection rate C_t/C_o is 0.82. Similar observation can be made at 3 NL/min^{-1} gas injection rate.

The maximum decrease of C_t/C_o between volume fraction of 0.1 and 0.15 is 10 percent.

4.2.2 Bottom Injection of Gas

In these experiments air is injected from top, one hole bottom which is at the centre of bottom plate. The water volume is taken 5.5 like for all the experiments reported in this section.

4.2.2.1 Influence of Gas Flow Rate

Figure 4.4 shows the variation of fractional concentration of benzoic acid in water resulting due to its transfer into the 550 ml oil (ϕ = 0.1) vs. time for various gas injection rate and Fig. 4.5 for 875 ml oil (ϕ = 0.15) and Fig. 4.6 for 1100 ml oil (ϕ =.0.2).

The experimental set-up is shown in Figure. It can be seen in the figures that as gas flow rate increases C_t/C_o decreases which implies increased transfer of benzoic acid to oil.

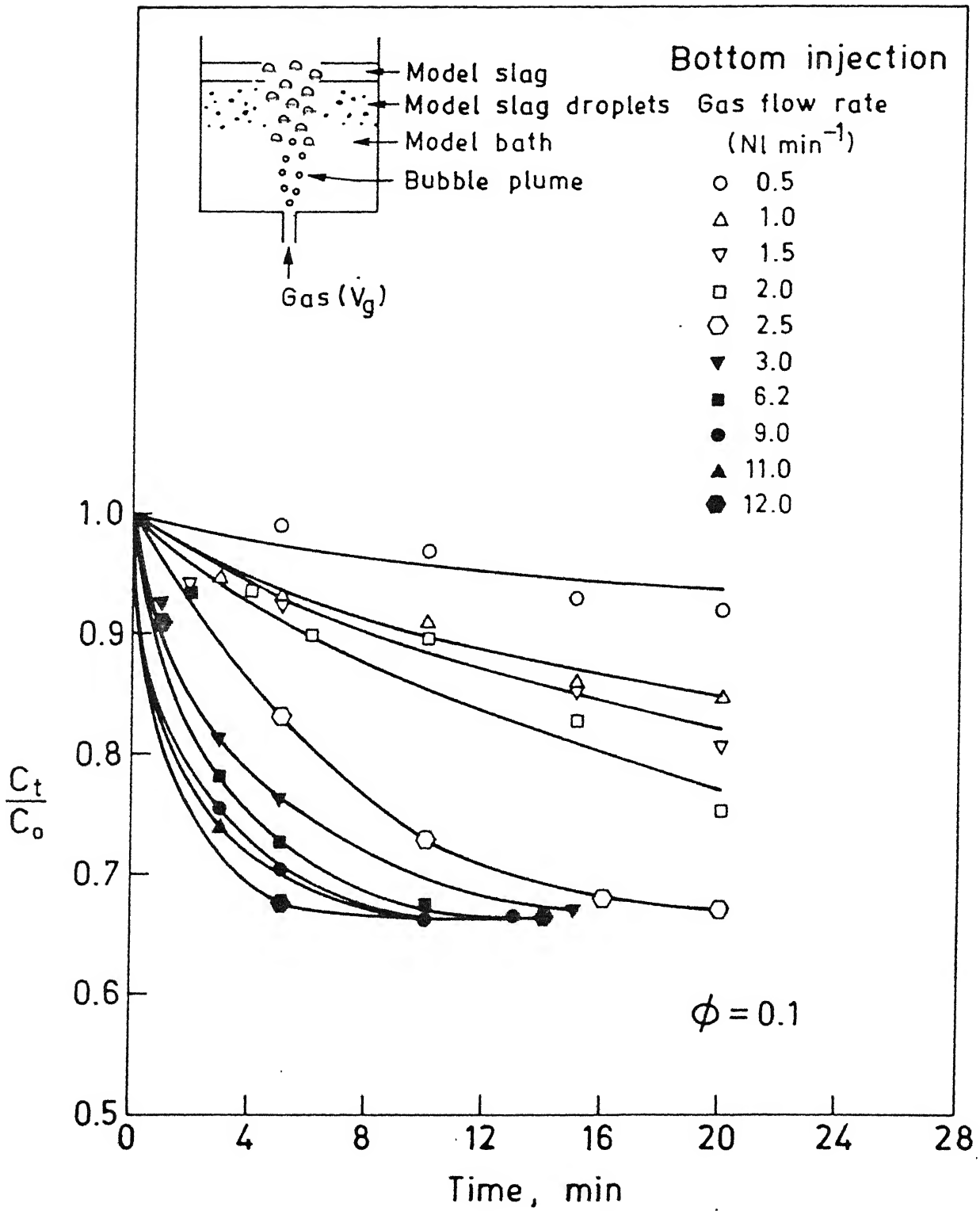

Fig. 4.4 : Fractional change of concentration of benzoic acid in water vs. time during bottom injection at various gas flow rate and for volume fraction of slag 0.1.

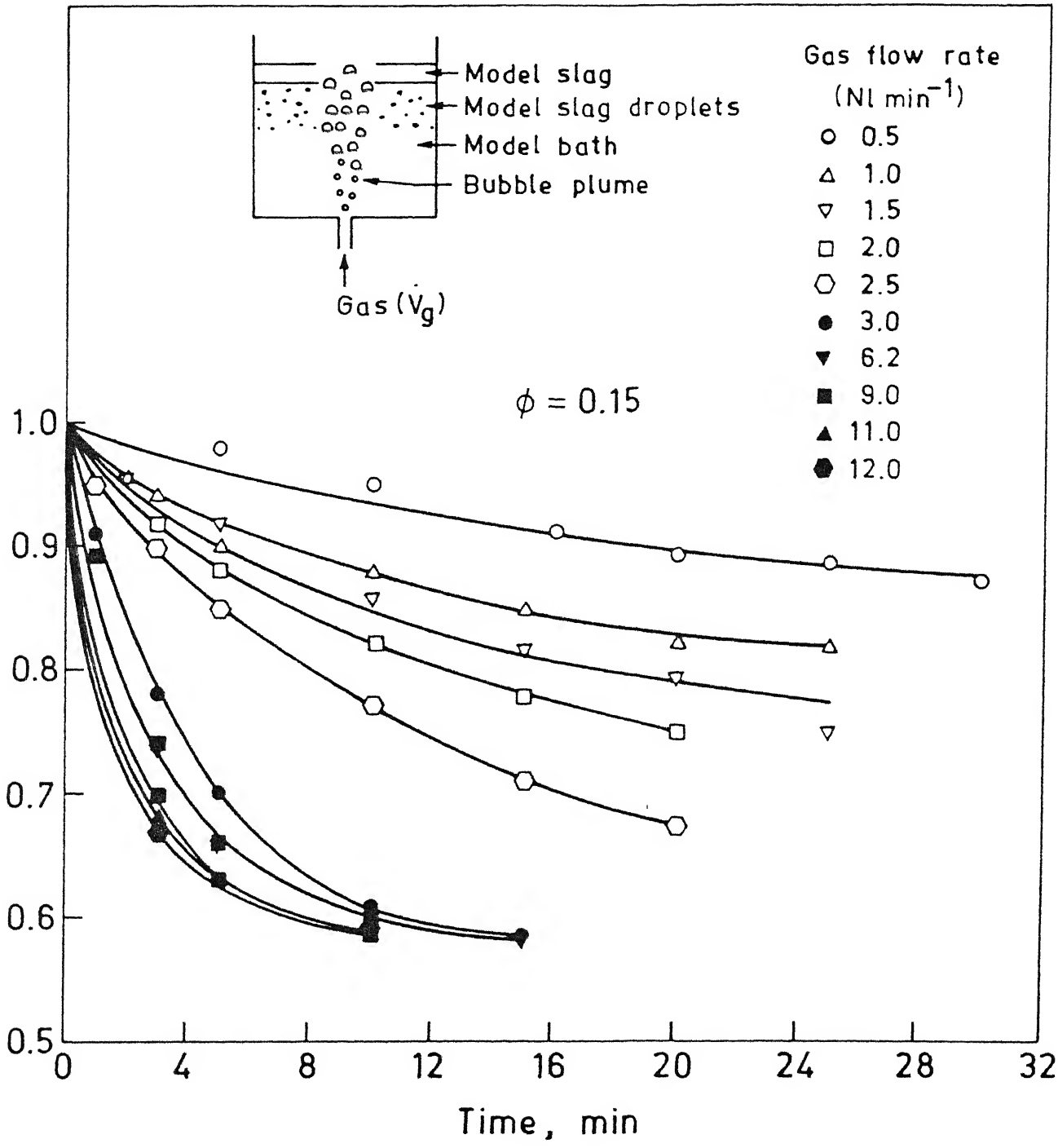

Fig. 4.5 : Fractional change of concentration of benzoic acid in water vs. time during bottom injection at variou gas flow rate and for volume fraction of slag 0.15.

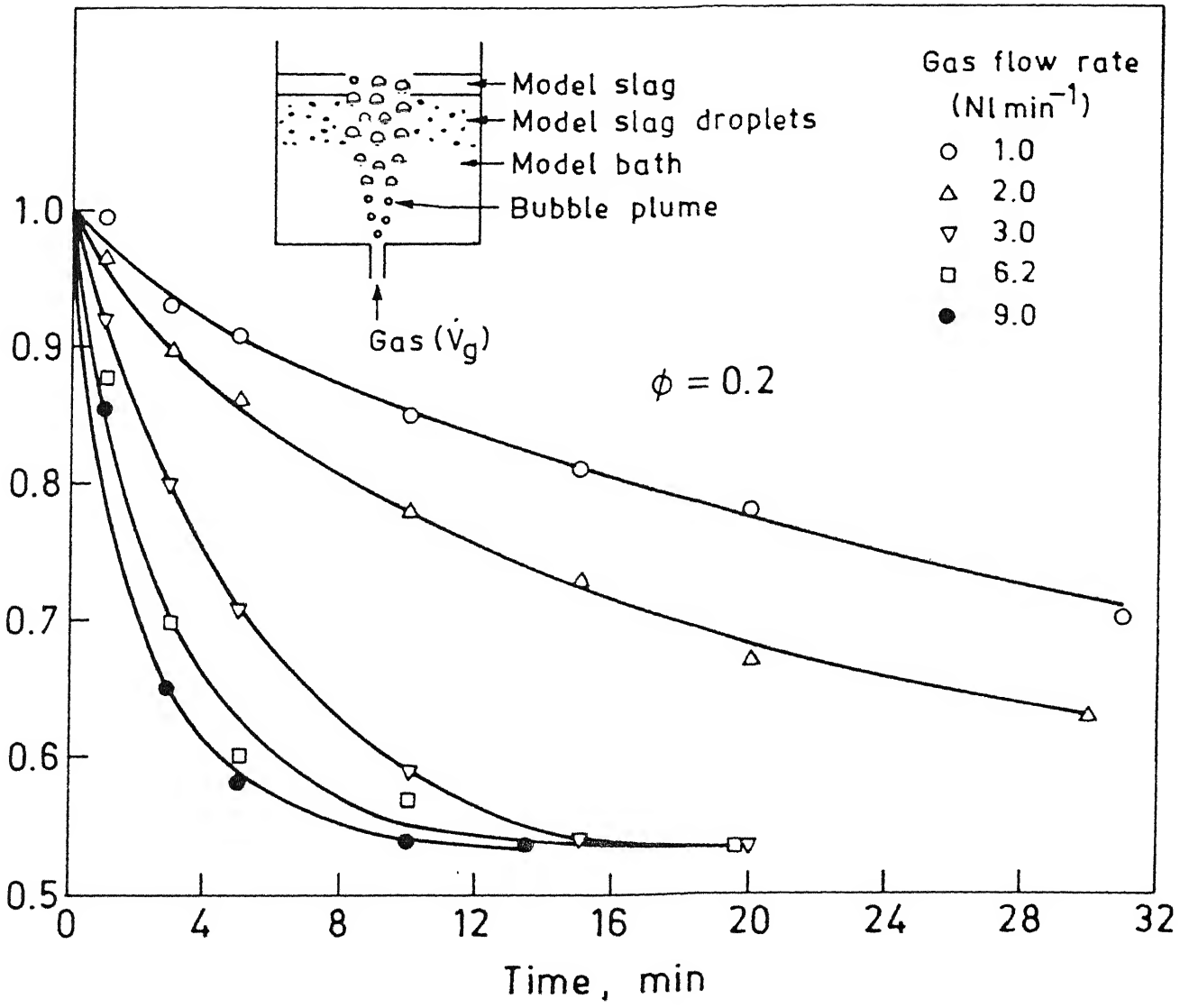

Fig. 4.6 : Fractional change of concentration of benzoic acid in water vs. time during bottom injection at various gas flow rate and for volume fraction of slag 0.2.

For example consider the value of C_t/C_o in Fig. 4.4 at 15 minutes for various gas flow rate. This value is 0.93 at 0.5 NL/min , 0.86 at 1 NL/min , 0.849 at 1.5 NL/min , 0.675 at 2 NL/min , 0.67 at 2.5 NL/min , 0.67 at 3 NL/min , 0.67 at 6.2 NL/min , 0.67 at 9 NL/min , 0.67 at 11 NL/min , 0.67 at 12 NL/min^{-1}.

It can be seen in the above three figures for high gas flow rate 2 NL/min after some time, there is no change in C_t/C_o. This lowest value of C_t/C_o is taken as equilibrium value. Similar observation can be made in Figs. 4.5 and 4.6.

4.2.2.2 Influence of Volume Fraction of Slag

Figure 4.7 compares the influence of slag volume on the change of fractional concentration of benzoic acid in water with respect to time for different gas flow rate, i.e. 1 NL/min and 3 NL/min .

It can be seen in the figure that increase in slag volume decreases the C_t/C_o for all times and at all gas injection rate.

For example consider the value of C_t/C_o in Fig. 4.7 at 15 minutes for gas flow rate 1 NL/min and various volume fraction of slag, i.e. $\phi = 0.1$, $\phi = 0.15$ and $\phi = 0.2$.

The value is 0.866 for $\phi = 0.1$, 0.85 for $\phi = 0.15$ and 0.81 for $\phi = 0.2$. Similar observations can be made at 3 NL/min gas injection rate. The maximum decrease of C_t/C_o between volume fraction of 0.1 and 0.2 is 20 percent.

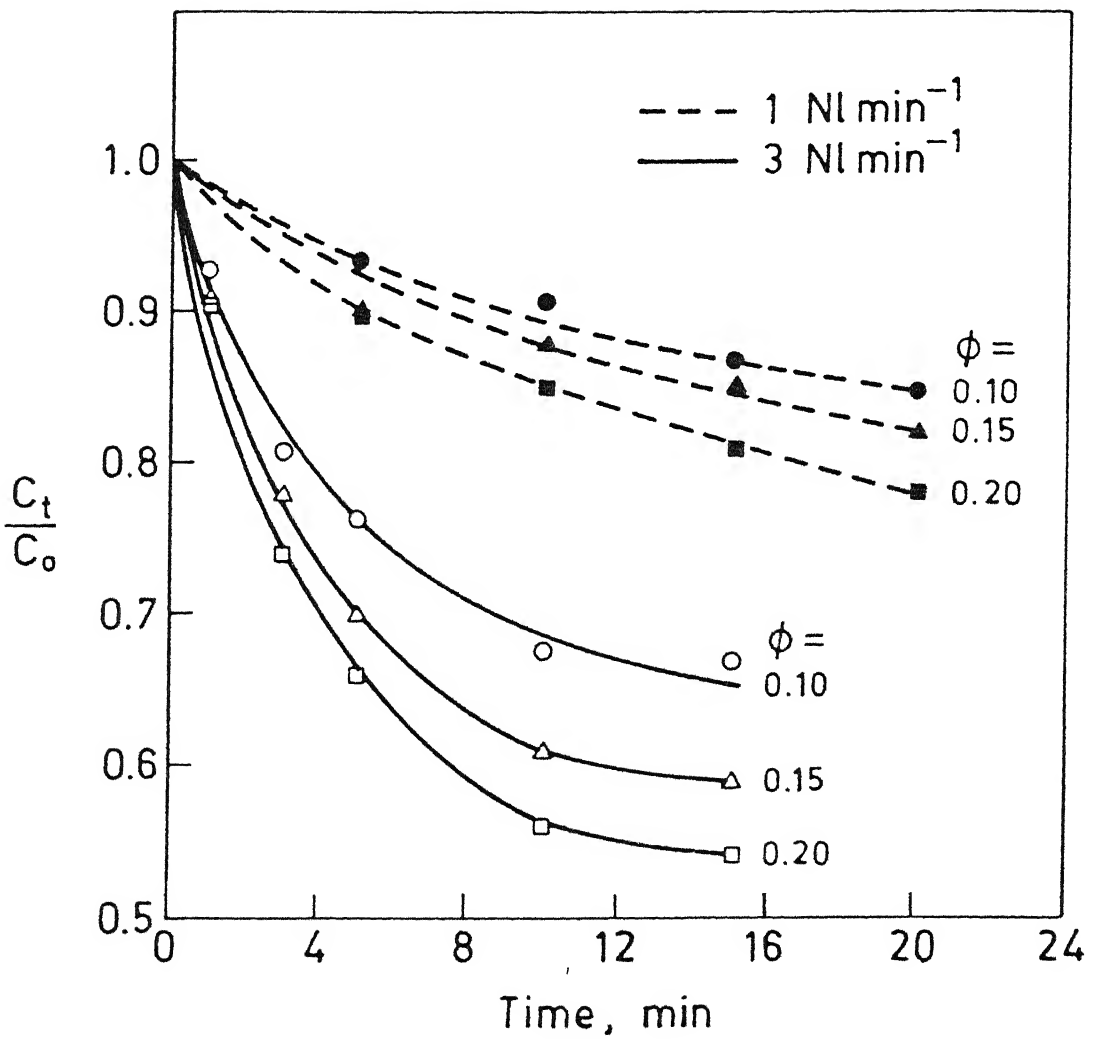

Fig. 4.7 : Fractional change of concentration of benzoic acid in water vs. time during bottom injection for 0.1, 0.15 and 0.2 volume fraction of slag at two gas flow rate (1 and 3 NL/min).

4.2.3 Comparison of Top and Bottom Injection

Figure 4.8 compares the change of C_t/C_o vs. time due to top and bottom injection for 550 ml model slag volume (ϕ = 0.1) and Fig. 4.9 for 875 ml slag volume (ϕ = 0.15). The gas injection rates are 1 NL/min^{-1} (dotted line) and 3 NL/min^{-1} (solid line) in both the figures.

Both figures show that for same gas flow rate and same time C_t/C_o is less for bottom injection than top injection which implies that in bottom injection transfer of benzoic acid from water to oil is more than top injection.

It can also observe in both the figure that the difference between top and bottom injection is more for 3 NL/min than 1 NL/min in C_t/C_o value.

Consider the value of C_t/C_o in Fig. 3.8 after 15 minutes and for 1 NL/min . C_t/C_o is 0.868 for top injection while it is 0.849 for bottom.

For the gas flow rate 3 NL/min after 10 minutes C_t/C_o is 0.74 for top injection and 0.675 for bottom injection. Similar observation can be made in Fig. 4.9.

4.2.4 INJECTION OF MODEL SLAG

4.2.4.1 Injection of Model Slag

Figure 4.10 shows the change of C_t/C_o for different depth of slag injector (B_i = Depth of nozzle/bath height) and for different nozzle diameter. Volume fraction of slag injected is 0.1.

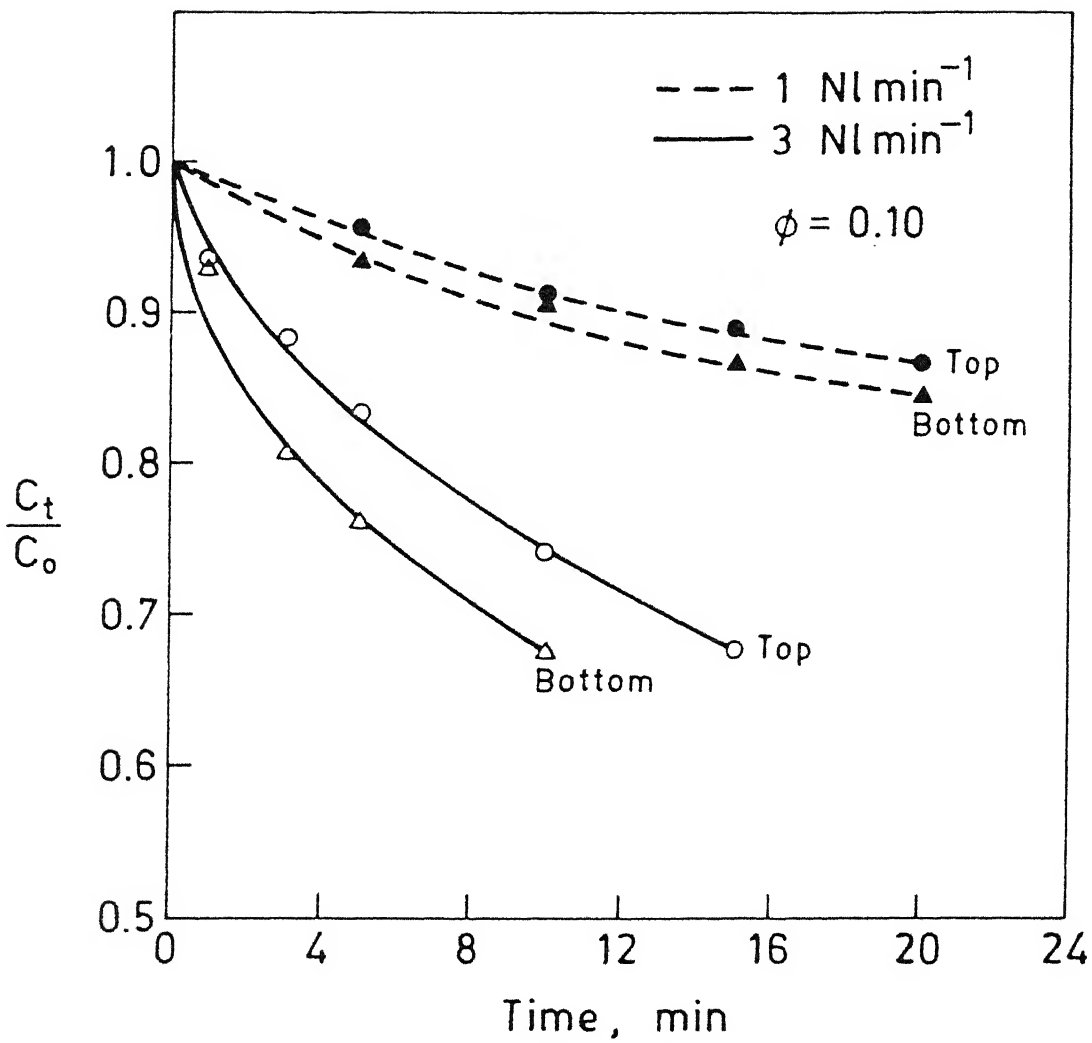

Fig. 4.8 : Fractional change of concentration of benzoic acid in water vs. time for top submergence lance (β = 0.5) and bottom injection at two gas flow rate (1 and 3 NL/min) and for volume fraction of slag 0.1.

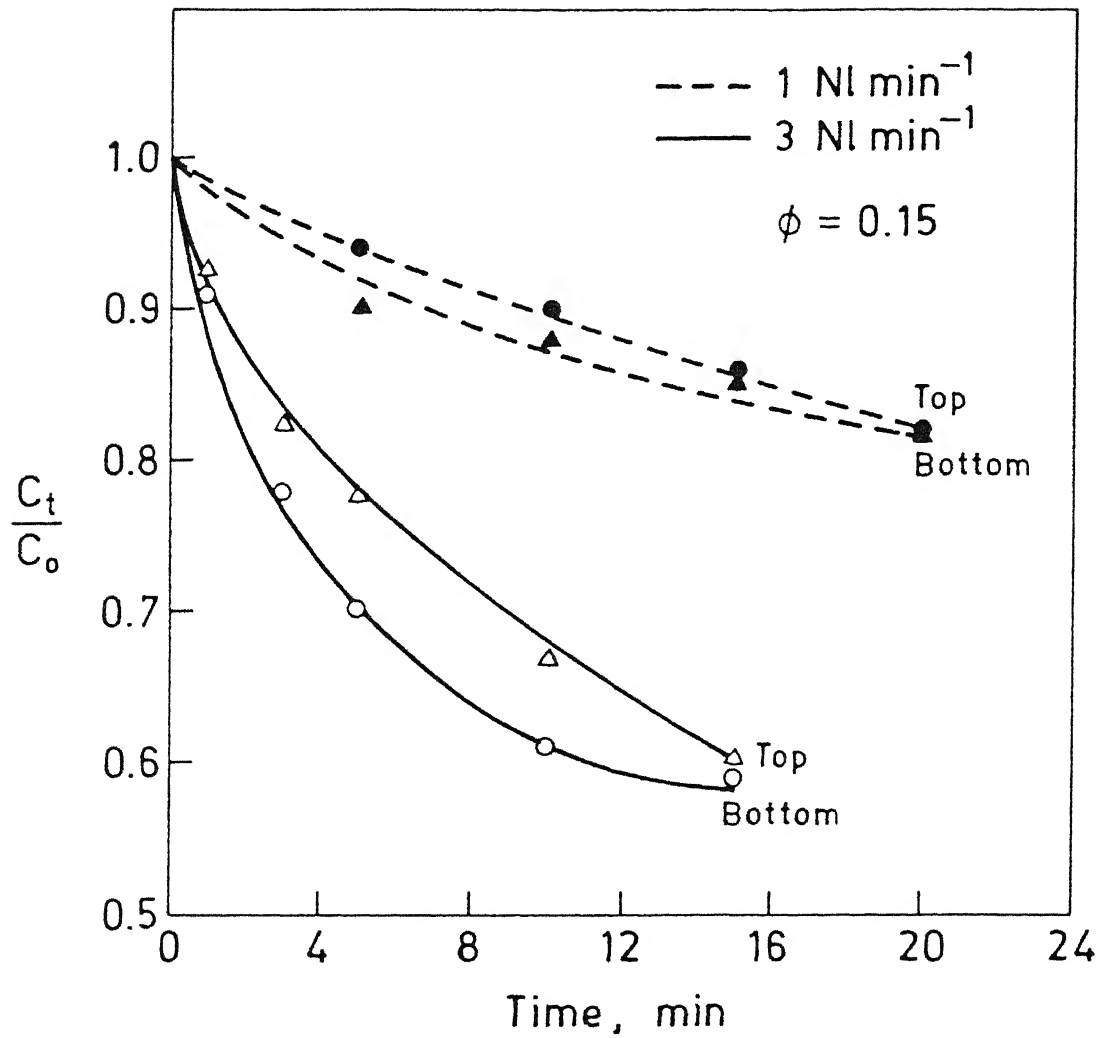

Fig. 4.9 : Fractional change of concentration of benzoic acid in water vs. time for top submergence lance (β = 0.5) and bottom injection at two gas flow rate (1 and 3 NL/min) and for volume fraction of slag 0.15.

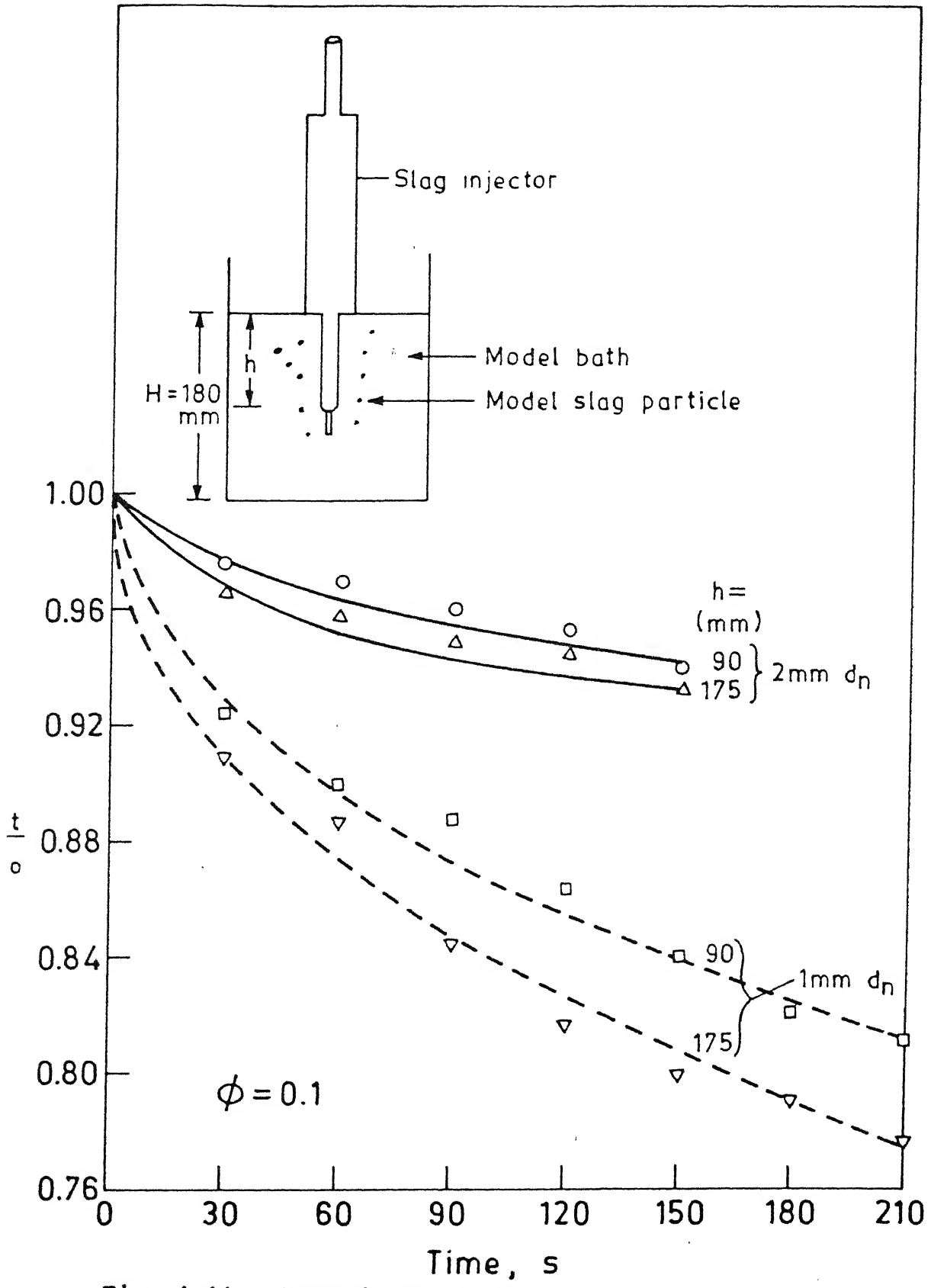

Fig. 4.11 : Fractional change of concentration of benzoic acid in water vs. time for injection of slag for two depth of submergence (0.5 and 0.95) and two diameter of nozzle (1 and 2 nm) and for volume

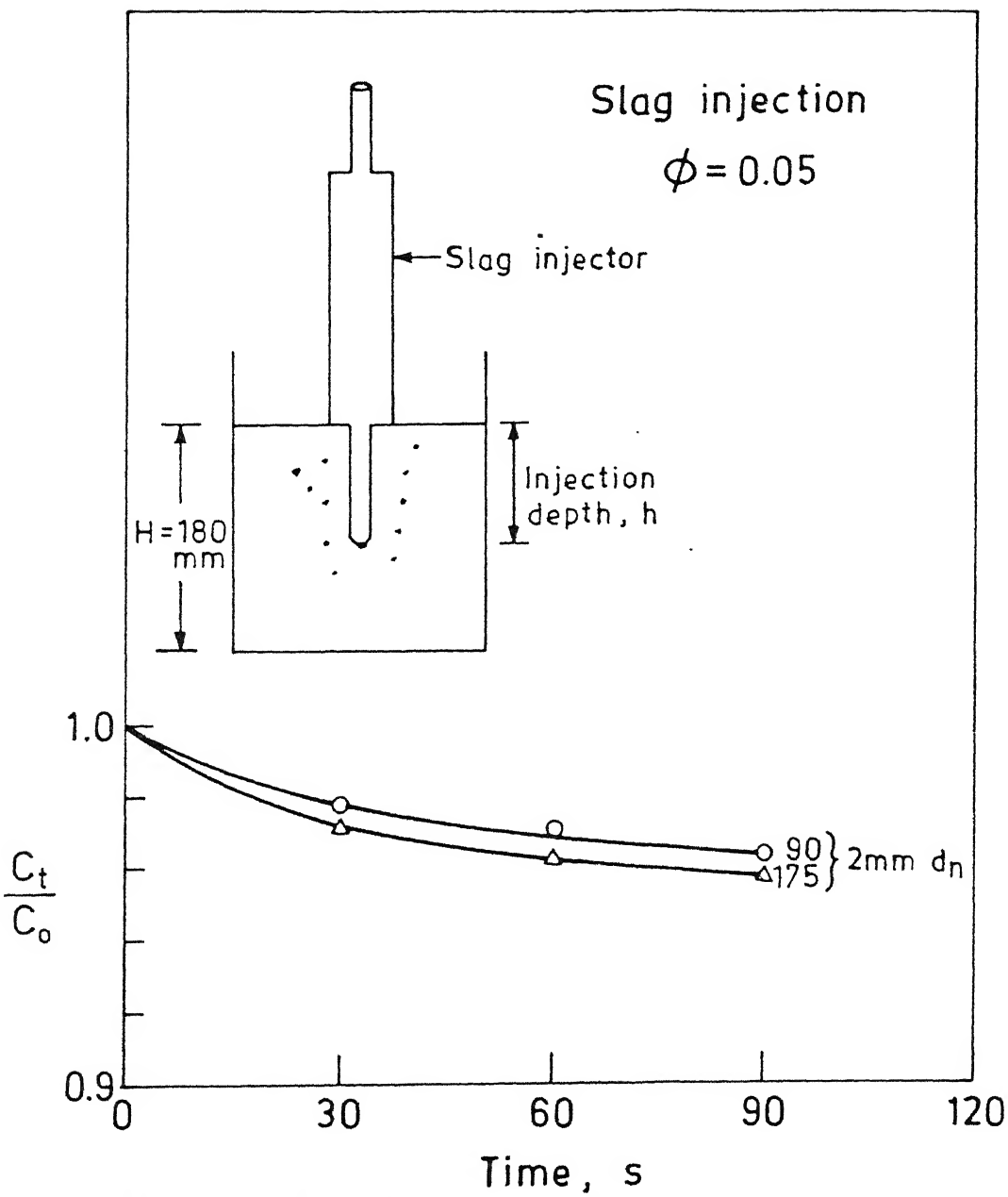

Fig. 4.10 : Fractional change of concentration of benzoic acid in water vs. time for injection of slag for two depth of submergence (0.5 and 0.95) and for 2 mm nozzle diameter and for volume fraction of slag 0.05.

Figure 4.11 shows the change of C_t/C_o for two depth of submergence of slag injector for 2 mm diameter nozzle. Volume fraction of slag is 0.05.

It can be seen that C_t/C_o decreases more as depth of submergence of slag injector increases and as nozzle diameter decreases.

After 90 sec, C_t/C_o is 0.969 for 2 mm nozzle diameter and it is 0.901 for 1 mm diameter nozzle for $\phi = 0.1$ at depth of submergence of slag injector = 0.5.

For the 1 mm nozzle diameter and for $\phi = 0.1$ for depth of submergence of injector nozzle = 0.5. C_t/C_o is 0.907 at 60 sec. while for depth of submergence = 0.95, it is 0.887.

4.3.2 Side Injection

In these experiments air is injected from side of the semicylindrical vessel by two nozzle of 2 mm diameter.

Figure 4.12 shows the variation of C_t/C_o of benzoic acid in water resulting due to its transfer into 1200 ml model slag ($\phi = 0.1$) vs. time for various gas injection rate.

The experimental set-up is shown in above figure. It can be seen in the figures that as the gas flow rate

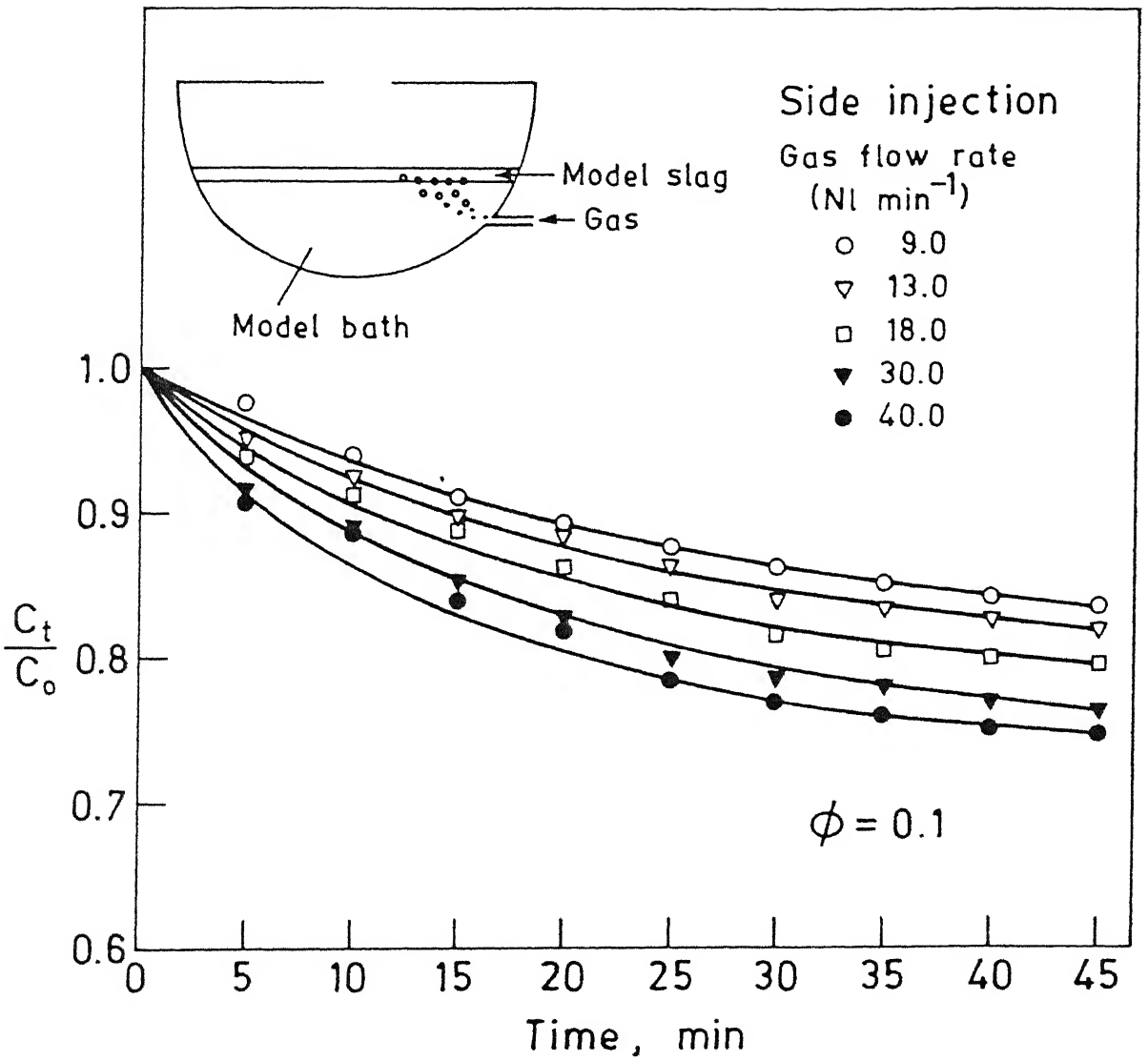

Fig. 4.12 : Fractional change of concentration of benzoic acid during side injection at various gas flow rate.

increases C_t/C_o decreases which implies increased transfer of benzoic acid to model slag phase.

For example consider the value of C_t/C_o in Fig. 4.12 at 30 minutes for various gas flow rate.

This value is 0.862 at 9 NL/min , 0.84 at 13 NL/min , 0.815 at 18 NL/min , 0.785 at 30 NL/min and 0.77 at 40 NL/min .

4.3 ANALYSIS OF RESULTS

According to equation (1.7) a plot of $\ln(\frac{C_t - C_e}{C_o - C_e})$ vs. time should give a straight line. All the results presented in Figures 4.13 to 4.20 are plotted according to equation (1.7). The straight line in these figures is drawn by the method of least square analysis. It can be seen in the figures that the equation (1.7) describes very well the result of the present investigation which suggests that diffusion of benzoic acid from water to oil phase is the rate controlling step. In this connection it must be noted that all diffusion process are accelerated by stirring, since stirring reduces the diffusion path on one hand and eleminates the concentration gradient on the other hand. The value of the rate constant determines the rapidity of the above mentioned transfer step and in the following the results are discussed in terms of the rate constant, i.e. K.

4.4 VARIATION OF RATE CONSTANT

4.4.1 Gas Injection

The results on the rate constant for gas injection and slag injection are separately presented.

In the figures 4.21 and 4.22 ln K is plotted against ln $\dot{V}_g$ for bottom and top injection respectively. The plot suggests that there exist 3 regions of dependence of rate constant (K) with gas injection rate. The results suggest further that K increases with increase in gas injection

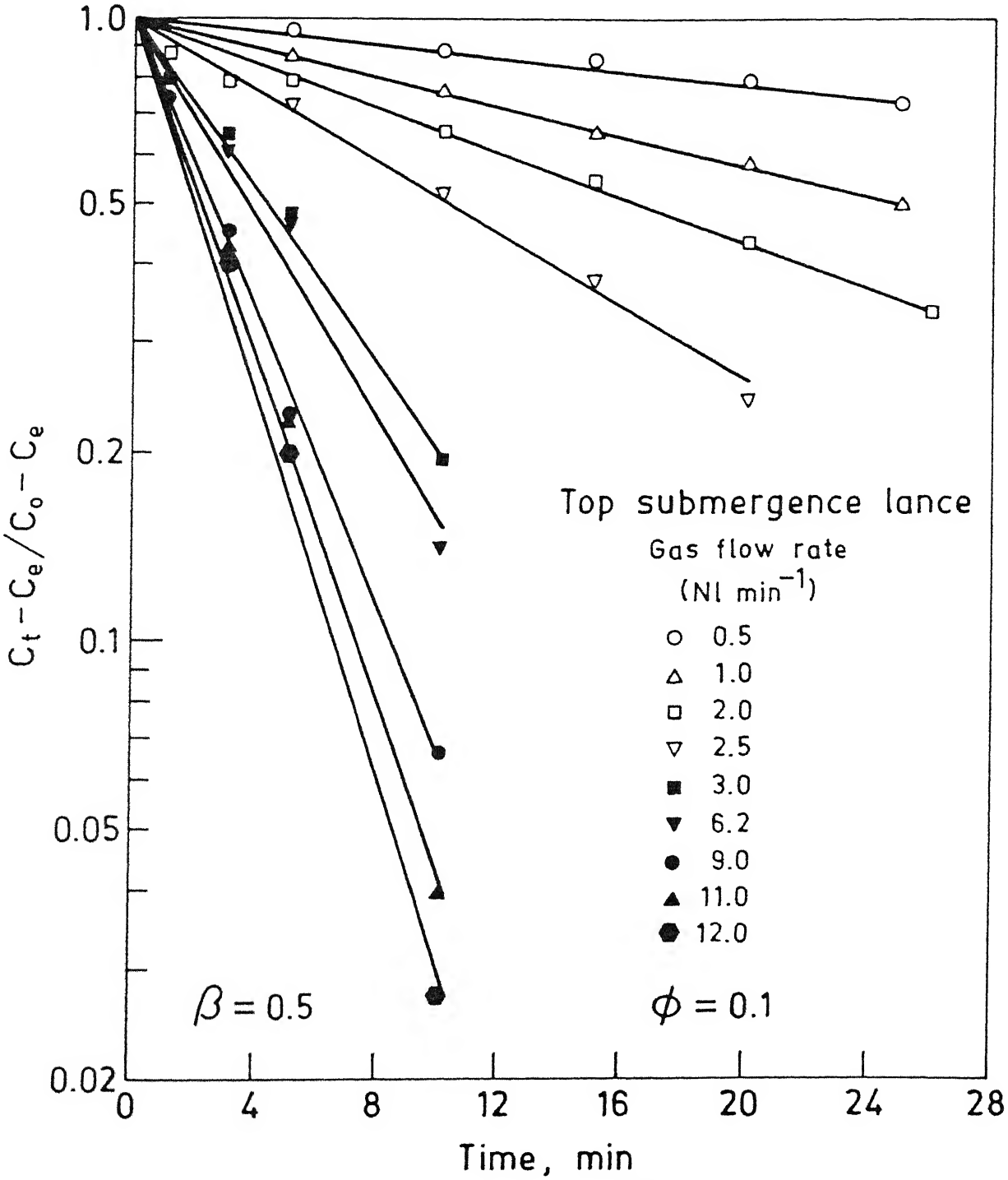

Fig. 4.13 : Variation of ln $\frac{C_t - C_e}{C_o - C_e}$ as a function of time for top submergence lance at ϕ = 0.1.

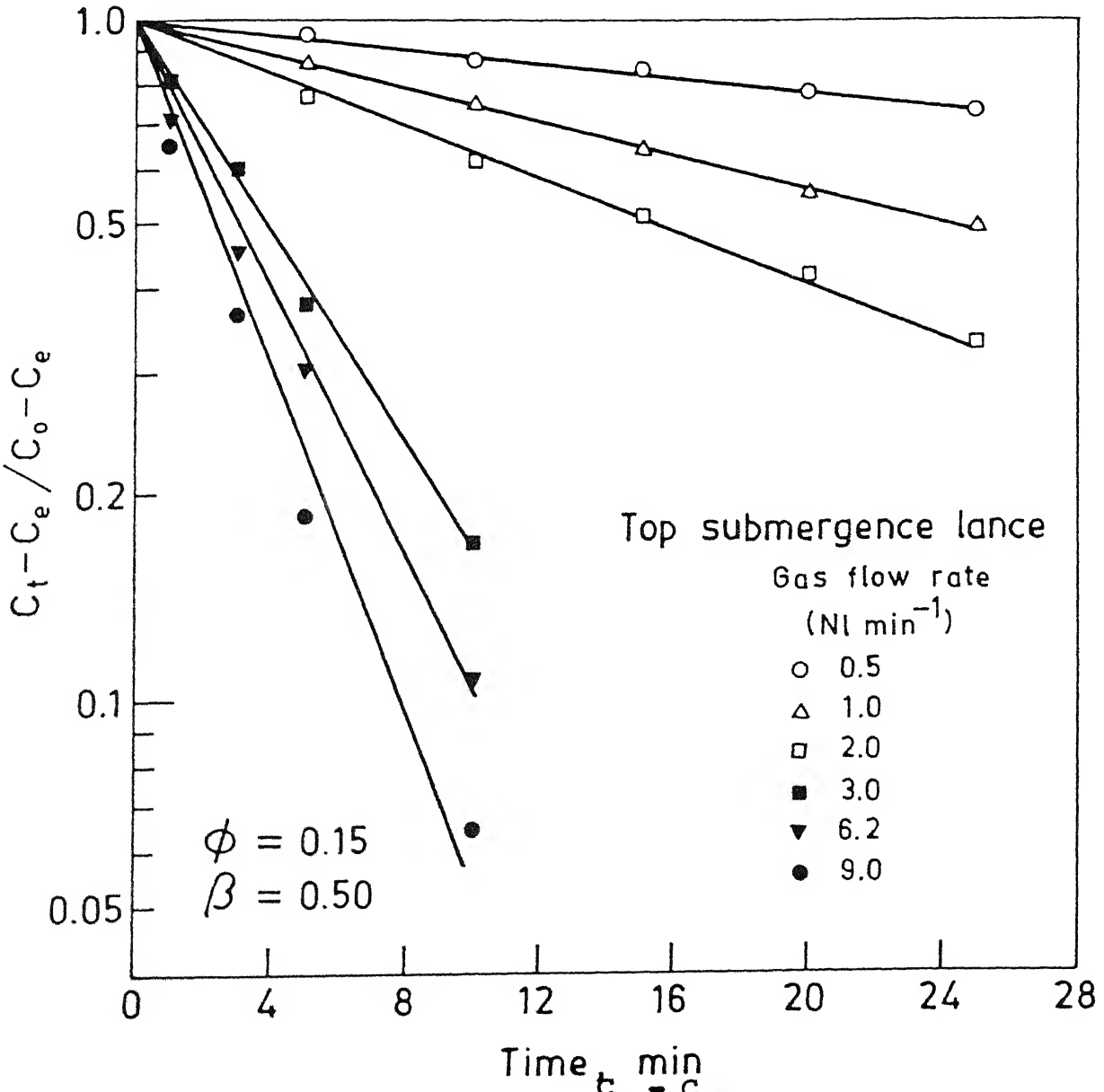

Fig. 4.14 : Variation of $\ln \frac{C_t - C_e}{C_o - C_e}$ as a function of time for top submergence lance ($\beta = 0.5$) at $\phi = 0.15$.

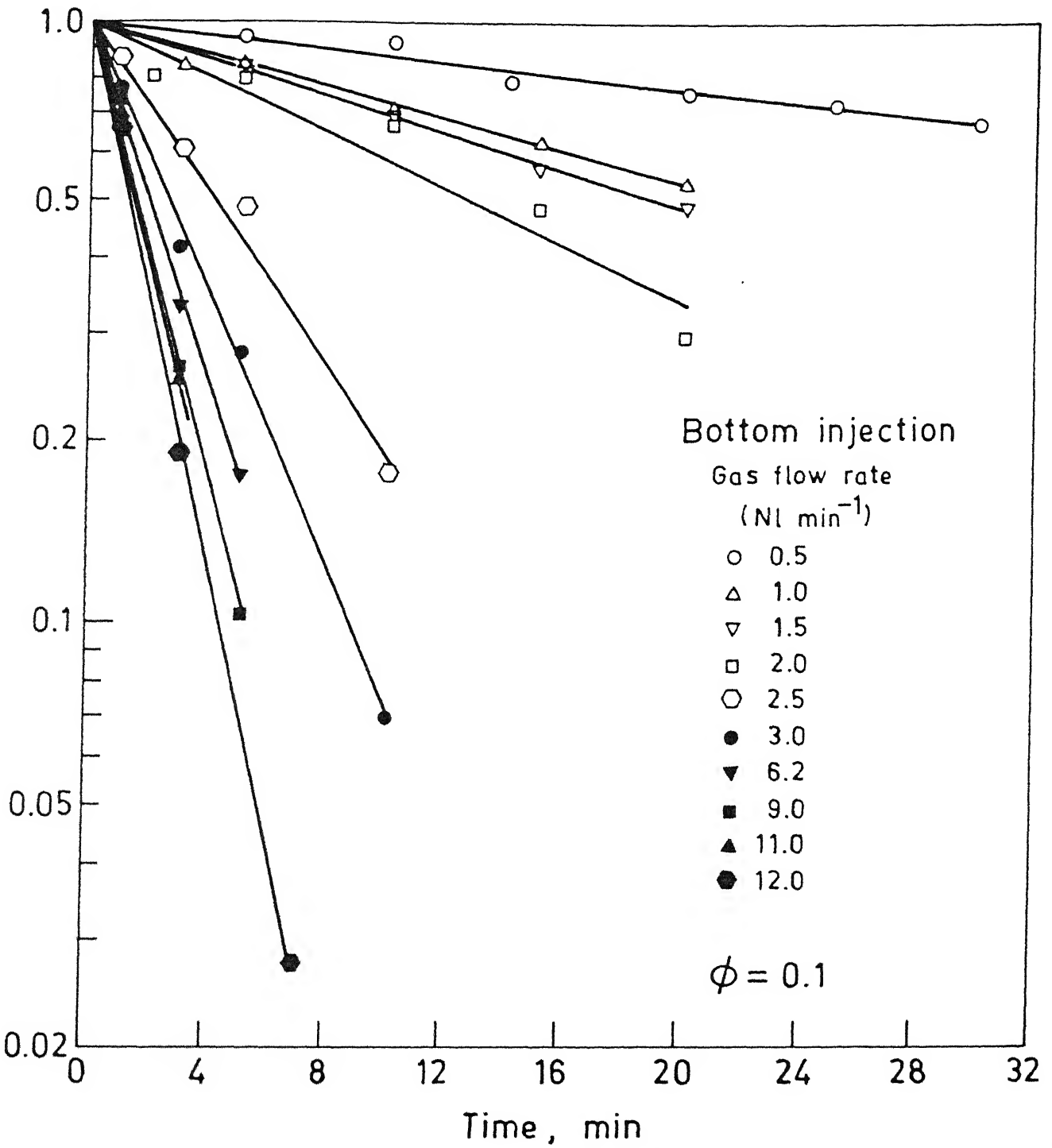

Fig. 4.15 : Variation of $\ln \frac{C_t - C_e}{C_o - C_e}$ as a function of time for bottom injection of gas at $\phi = 0.1$.

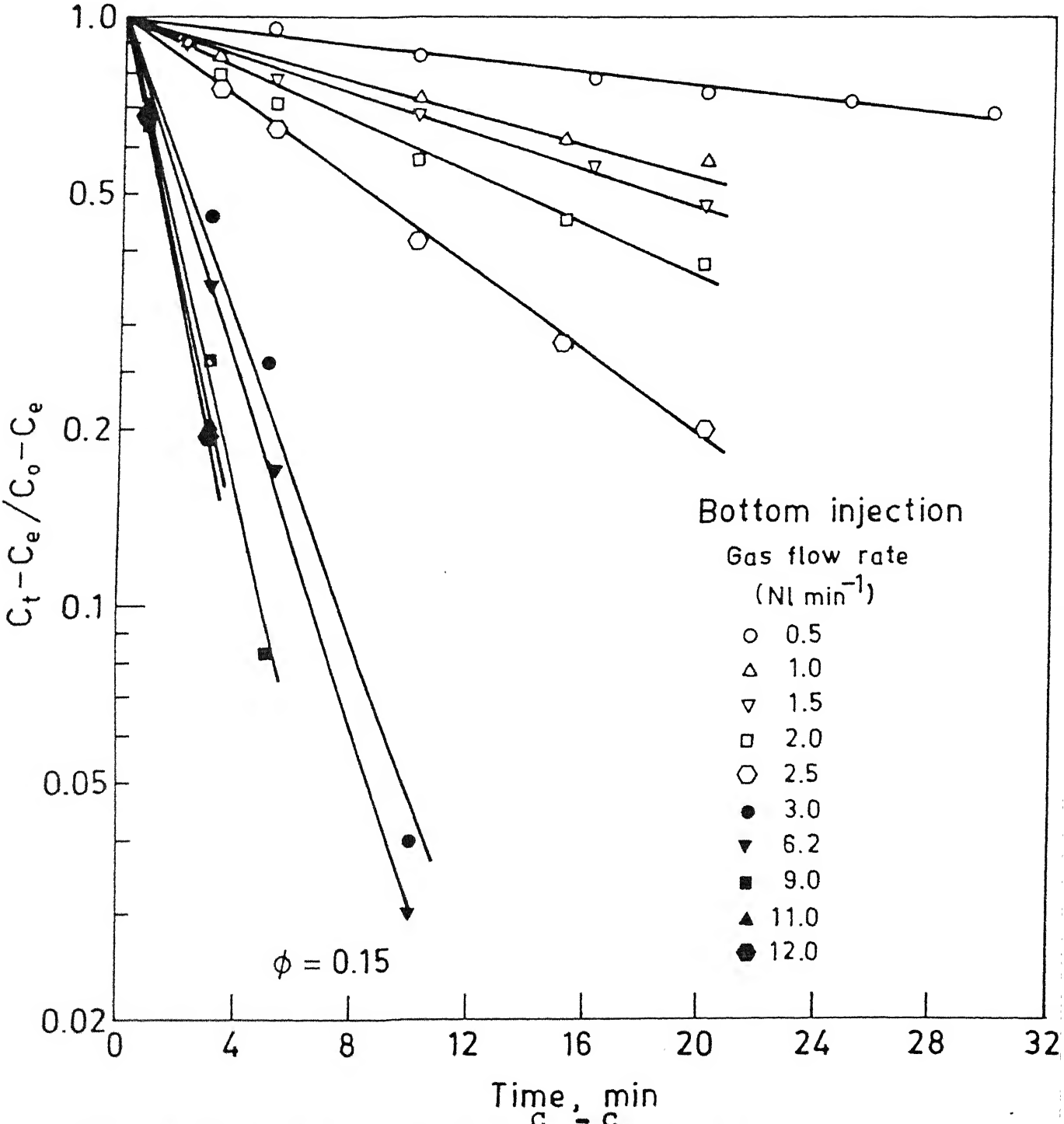

Fig. 4.16 : Variation of $\ln \frac{C_t - C_e}{C_o - C_e}$ as a function of time for bottom injection of gas at $\phi = 0.15$.

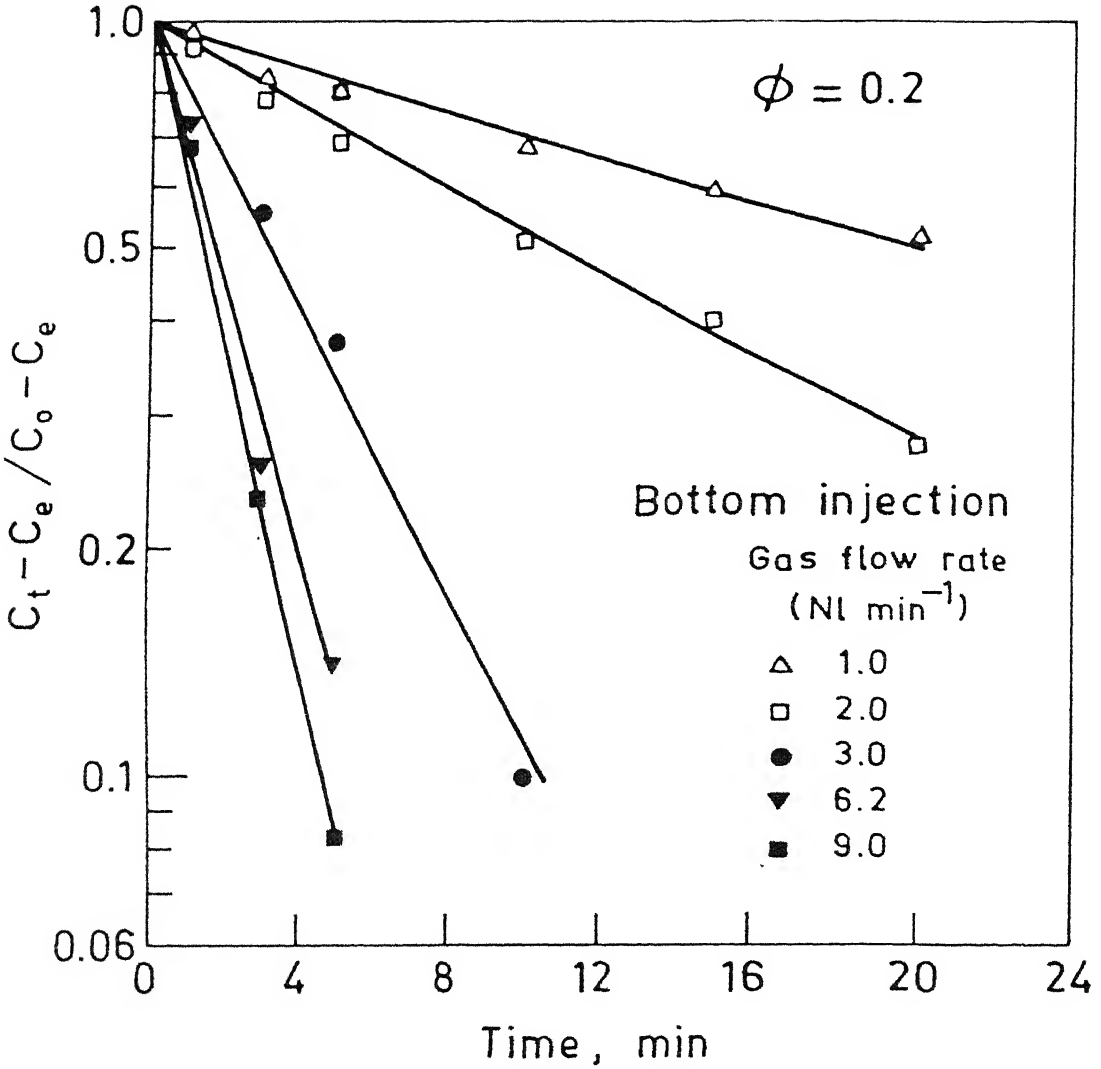

Fig. 4.17 : Variation of $\ln \frac{C_t - C_e}{C_o - C_e}$ as a function of time for bottom injection at $\phi = 0.2$.

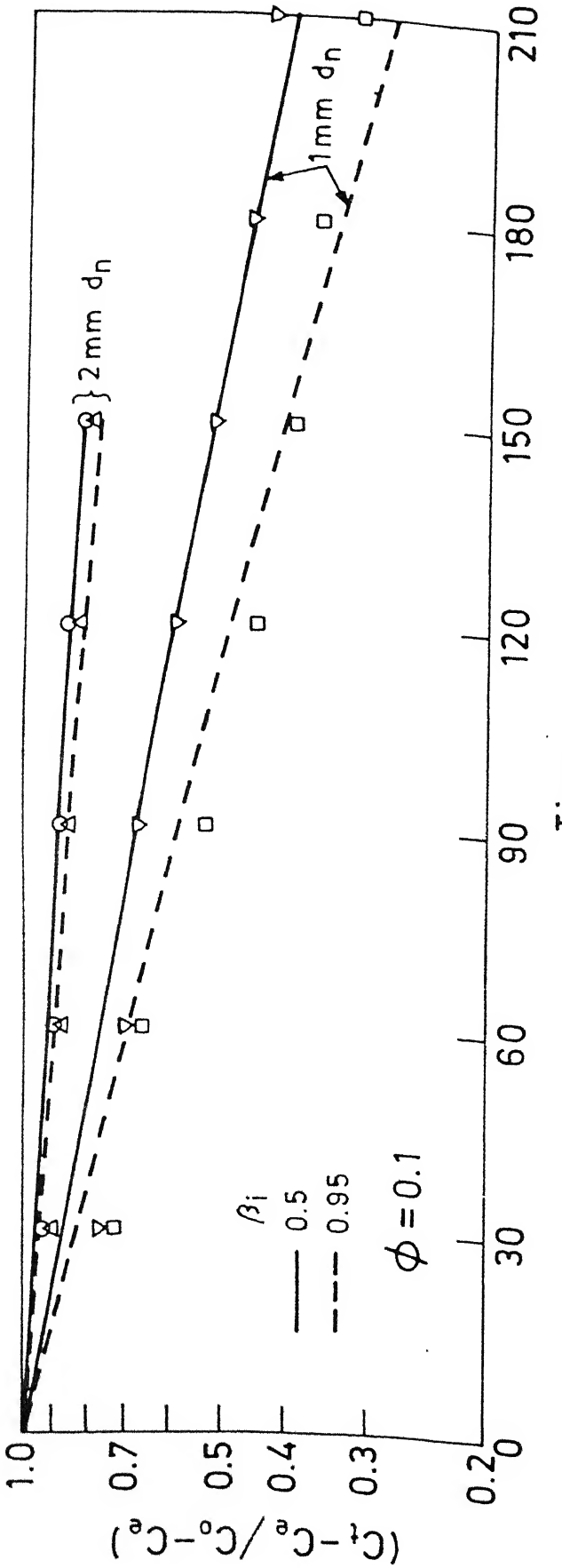

Fig. 4.18 : Variation of $\ln \frac{C_t - C_e}{C_o - C_e}$ as a function of time for injection of slag (volume fraction of slag = 0.1).

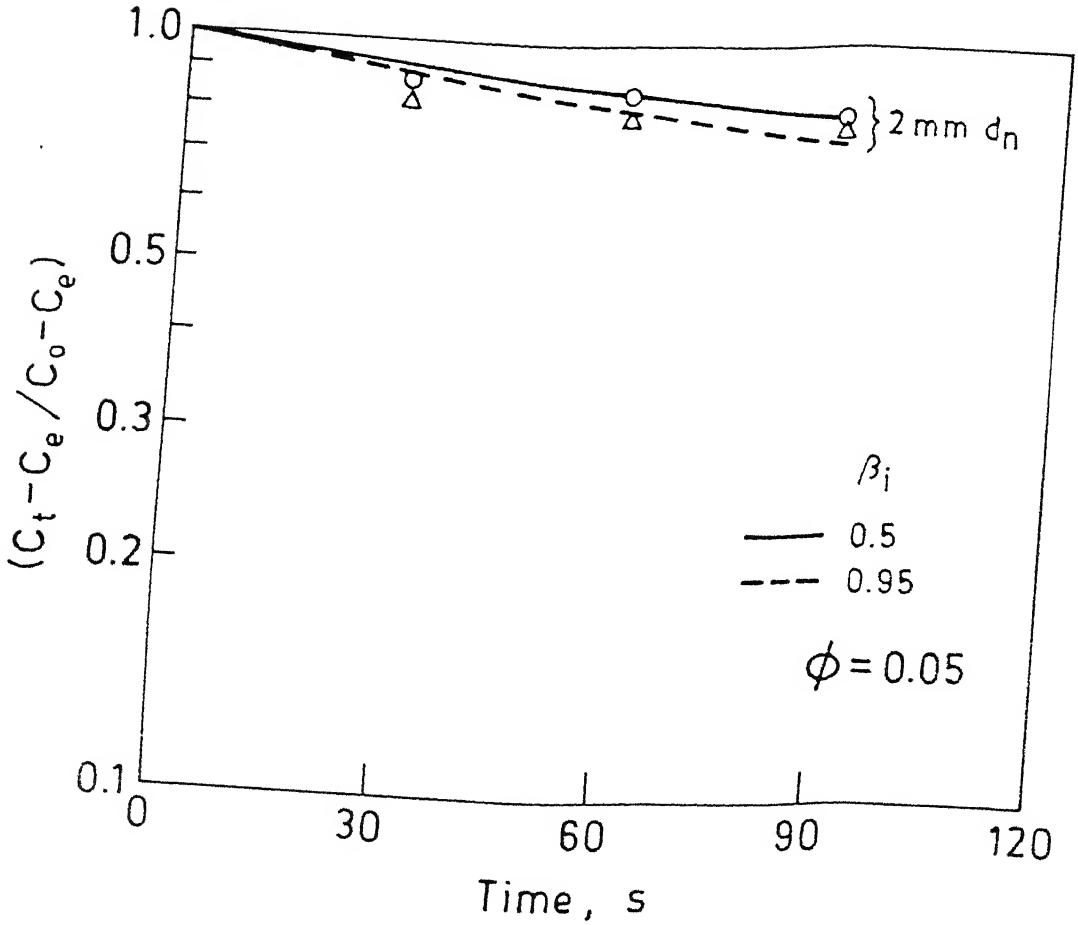

Fig. 4.19 : Variation of $\ln \frac{C_t - C_e}{C_o - C_e}$ as a function of time for injection of slag (volume fraction of slag = 0.05).

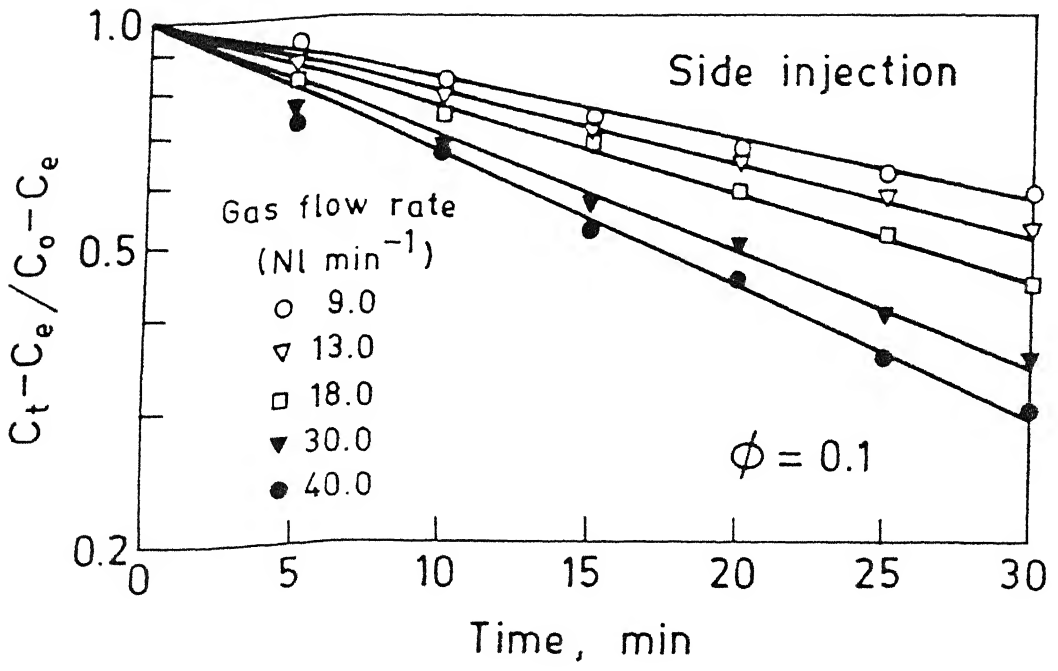

Fig. 4.20 : Variation of ln $\frac{C_t - C_e}{C_o - C_e}$ as a function of time for side injection.

rate and increase in volume fraction of slag, although the influence of later is very much less than that of former. Inspite of this K is treated in the following as a function of both the parameters, i.e. gas injection rate and volume fraction of slag. The following function has been used to obtain the empirical relationship:

$$K = \alpha (\dot{V}_g)^n \phi^m \qquad (4.1)$$

In the equation (4.1) α , n and m are constant. The value of these constant is determined by multiple regression analysis.

The following equations are obtained:

Bottom Injection:

For low flow rate region, i.e. $\dot{V}_g$ is less than 2 NL/min, NFr less than 0.668 and N'Fr less than 0.0547

$$K_b = 0.0488\ \dot{V}_g^{0.971}\ \phi^{0.252}\ \sigma = \pm\ 0.0051 \qquad (4.2)$$

For high flow rate region i.e. $\dot{V}_g$ is greater than 3 NL/min, NFr is greater than 0.668 and N'Fr greater than 0.072

$$K_b = 0.168\ V_g^{0.4312}\ \phi^{0.176}\ \sigma = \pm\ 0.0715 \qquad (4.3)$$

For top injection.

For low flow rate region, i.e. $\dot{V}_g$ is less than 2 NL/min, NFr less than 0.668 and N'Fr less than 0.00418

$$K_t = 0.0321\ \dot{V}_g^{0.899}\ \phi^{0.1244}\ \sigma = \pm\ 0.0027$$

For high gas flow rate region, i.e. V_g is greater than 3 NL/min. N_{Fr} greater than 0.668 and N'_{Fr} greater than 0.045

$$K_t = 0.135 \quad \dot{V}_g^{0.513} \quad \phi^{0.186} \qquad \sigma = \pm 0.0207 \tag{4.5}$$

In Fig. 4.2 K and $\dot{V}_g$ is plotted in ln = ln graph for volume fraction of slag 0.1 for side injection. Least square line is

$$K = 5.5 \times 10^{-3} \quad \dot{V}_g^{0.5544} \qquad \sigma = \pm 0.00033 \tag{4.6}$$

The above equations are used to construct the lines reported in the figures 4.21, 4.22, 4.23, 4.24 and 4.25. In Equation 4.2 to 4.6, K is in min^{-1} and $\dot{V}_g$ is in NL/min.

4.4.2 Slag Injection

The value of rate constant are listed in Table 4.3. From the table, it can be seen that K increases with increase in depth of submergence of slag injector into the metal bath and by decrease in nozzle diameter for the same amount of slag. An increase in the injected amount of slag decreases the value of K. This may be due to the depleted region of concentration of benzoic acid in water.

4.5 INFLUENCE OF GAS FLOW RATE ON RATE CONSTANT

Figure 4.21 shows the variation of lnK with $\ln\dot{V}_g$ for bottom injection while figure 4.22 is for top injection. The equations (4.2) and (4.4) at constant ϕ are used to draw line for regime I.

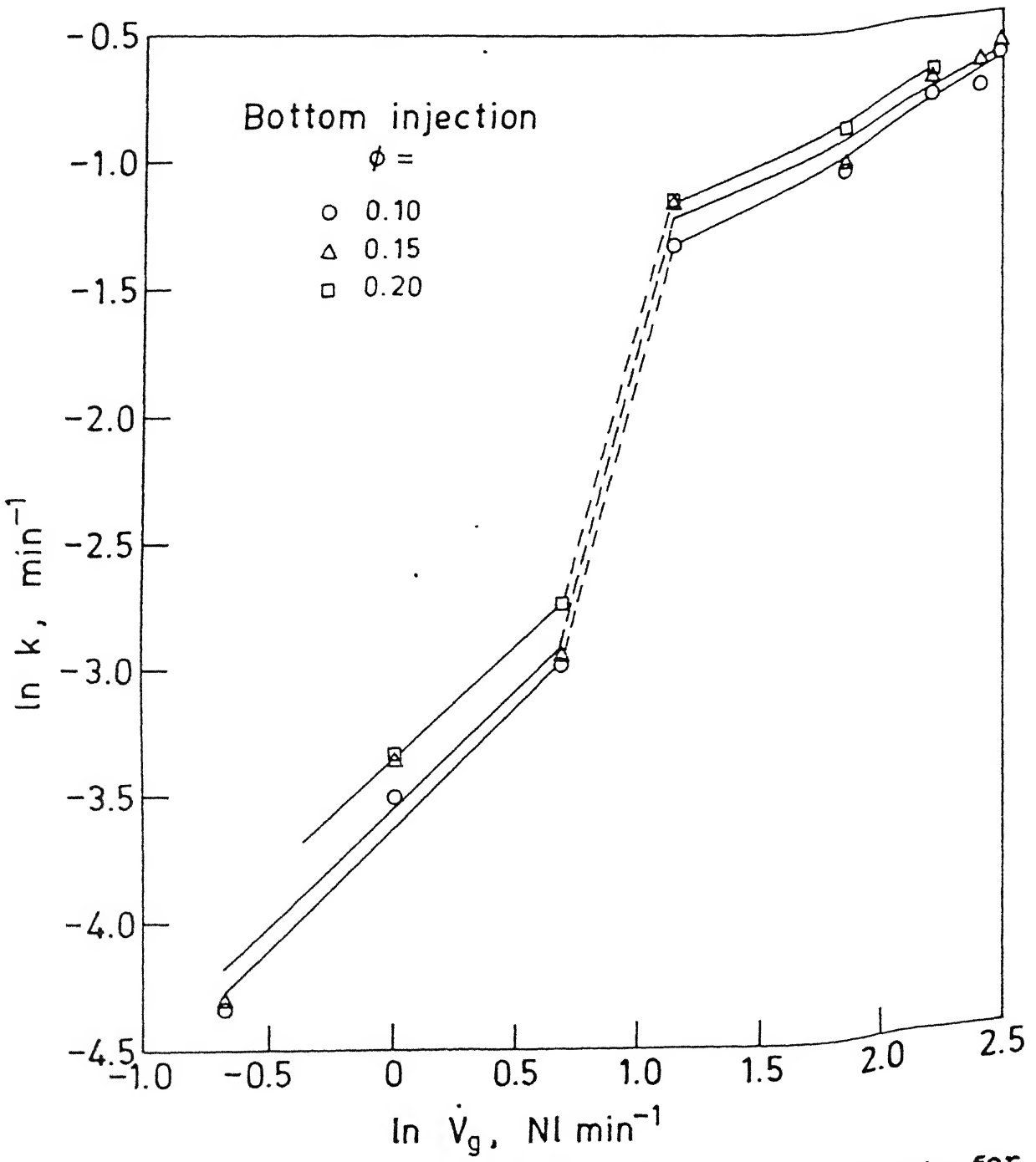

Fig. 4.21 : A plot K as a function of gas flow rate for different volume fraction of slag.

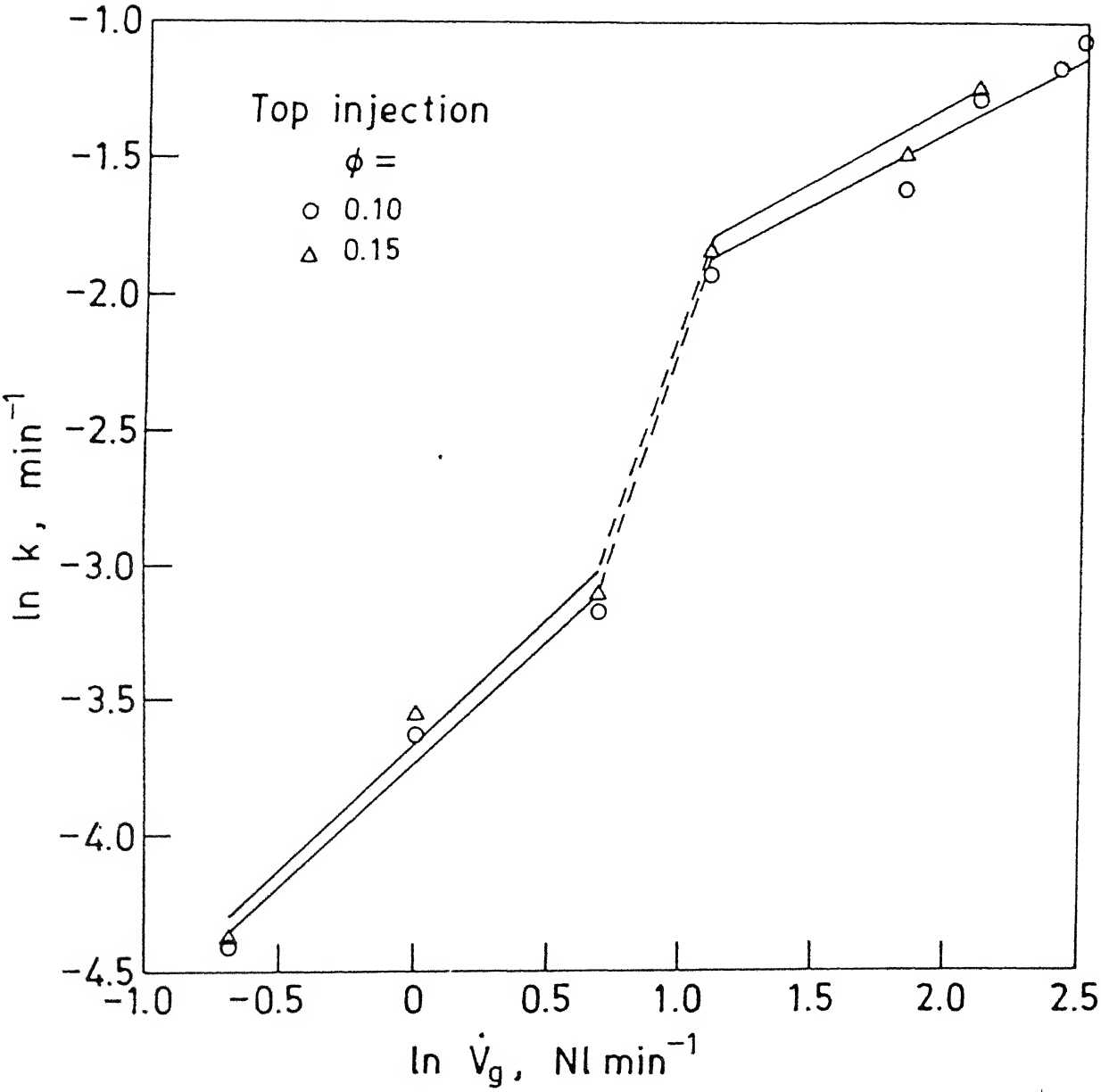

Fig. 4.22 : A plot as a function of gas flow rate for different volume fraction of slag.

$$K_b = 0.0273\ (\dot{V}_g)^{0.971} \quad \text{for } \phi = 0.1 \qquad (4.7)$$

$$K_b = 0.03\ (\dot{V}_g)^{0.971} \quad \text{for } \phi = 0.15 \qquad (4.8)$$

$$K_b = 0.032\ (\dot{V}_g)^{0.0971} \quad \text{for } \phi = 0.2 \qquad (4.9)$$

$$K_t = 0.024\ (\dot{V}_g)^{0.899} \quad \text{for } \phi = 0.1 \qquad (4.10)$$

$$K_t = 0.0254\ (\dot{V}_g)^{0.899} \quad \text{for } \phi = 0.15 \qquad (4.11)$$

Equations (4.3) and (4.5) at constant ϕ are used to draw line for regime III

$$K_b = 0.1678\ (\dot{V}_g)^{0.4312} \quad \text{for } \phi = 0.1 \qquad (4.12)$$

$$K_b = 0.18\ (\dot{V}_g)^{0.4312} \quad \text{for } \phi = 0.15 \qquad (4.13)$$

$$K_b = 0.1895\ (\dot{V}_g)^{0.4312} \quad \text{for } \phi = 0.1 \qquad (4.14)$$

$$K_t = 0.088\ (\dot{V}_g)^{0.513} \quad \text{for } \phi = 0.1 \qquad (4.15)$$

$$K_t = 0.095\ (\dot{V}_g)^{0.513} \quad \text{for } \phi = 0.15 \qquad (4.16)$$

These equations are used to construct the lines shown in the figure. K_b and K_t are low in this region because no oil droplets are entrained into water (see photographs (1 and 4) and the interface between oil and water phases is close to plance surface except for the very weak wave motion of the interface near the edge of plume and due to pushing by the bubble when it reaches the interface.

The effect of stronger agitation on the mass transfer begins to decreases because the mass transfer enhancement mechanism, i.e. size and number of oil droplets stabilizes.

Then recirculating and entraining depth of droplets in the liquid bath are the major parameters responsible for increasing the mass transfer instead of the number of entrained oil droplets. Increase of gas flow rate increases the entrainment depth of oil droplets into water (See photographs 2,3 and 5,6) without much affecting the size distribution of the oil droplets produced due to the gas injection.

The region II is characterized by an abrupt increase in the rate constant. This abrupt change of the dependence can be explained by the observation that the oil layer near the edge of the plume eye continuously forms oil ligments and then breaks up into the water. This phenomena increases the oil/water interfacial area. This critical gas flow rate defines the boundary between regime I and region II. It is at this gas flow rate that oil droplets are formed and the entrainment of these droplets into the bulk liquid phase starts to occur.

In the region III, K_b and K_t values are significantly higher than those of region 1. In this region, nearly the entire oil layer breaks down into oil droplets

without forming oil ligments near the edge of plume eye right after gas injection and the penetration of oil droplets deep into the water bath occurs. Further the influence of gas injection rate on increase in K in this region is very much less than that of region I (see the exponent of $\dot{V}_g$, i.e. eq. 4.7 to 4.11 and 4.12 to 4.16). This observation is valid for top as well as bottom gas injection.

Similar three regime has been found by Seon-Hyo Kimetal[6] in gas injection experiment. According to them, with increasing oil volume ratio, the intermediate regime becomes narrower and finally too narrow to define. They used 3.3 and 6% slag in their experiments. Increase in oil % from 3.3 to 6% made the intermediate region narrower. In the present experiments, the oil volume is 10-20% of the bath value, i.e. much higher than that of used by Seon et al. It is quite possible that for the range of oil percent. . used in this study, the intermediate region is extremely narrowed and ultimately very difficult to define as the experimental results in Fig. 4.25 show.

If the slag volume is less, than the injected gas will pass through slag layer without much affecting the slag layer. So the oil entrainment will not effective by gas injection. But if slag volume is more, i.e. slag layer is thick passing gas will effectively produce circulation

motion in the slag layer so oil entrainment will occur early in this case, so the intermediate will become narrow. These ideas are illustrated in the Fig. 4.23.

4.6 SIDE INJECTION

Figure 4.24 is a plot between lnK and $\ln\dot{V}_g$ for $\phi = 0.1$ by equation (4.6). This graph shows the linear variation of lnK with $\ln\dot{V}_g$. Here no oil entrainment has been found so there is no abrupt increase of K with $\dot{V}_g$. Value of K increases with gas flow rate because there is more circulation of liquid so fresh liquid always come in contact with slag layer.

4.7 VARIATION OF RATE CONSTANT WITH ϕ

Variation of K with ϕ for different gas flow rate and for top and bottom injection of gas is shown in Fig. 4.25. Equations (4.2) and (4.4) is used to draw the line for low gas flow rate region for bottom and top respectively.

There is increase in K_b and K_t by increasing the volume fraction of slag because as the volume fraction of slag increases the plume eye diameter becomes less so interfacial area for mass transfer becomes more.

For high gas flow rate region , equation (4.3) and equation (4.5) is used to draw the line for bottom and top injection respectively.

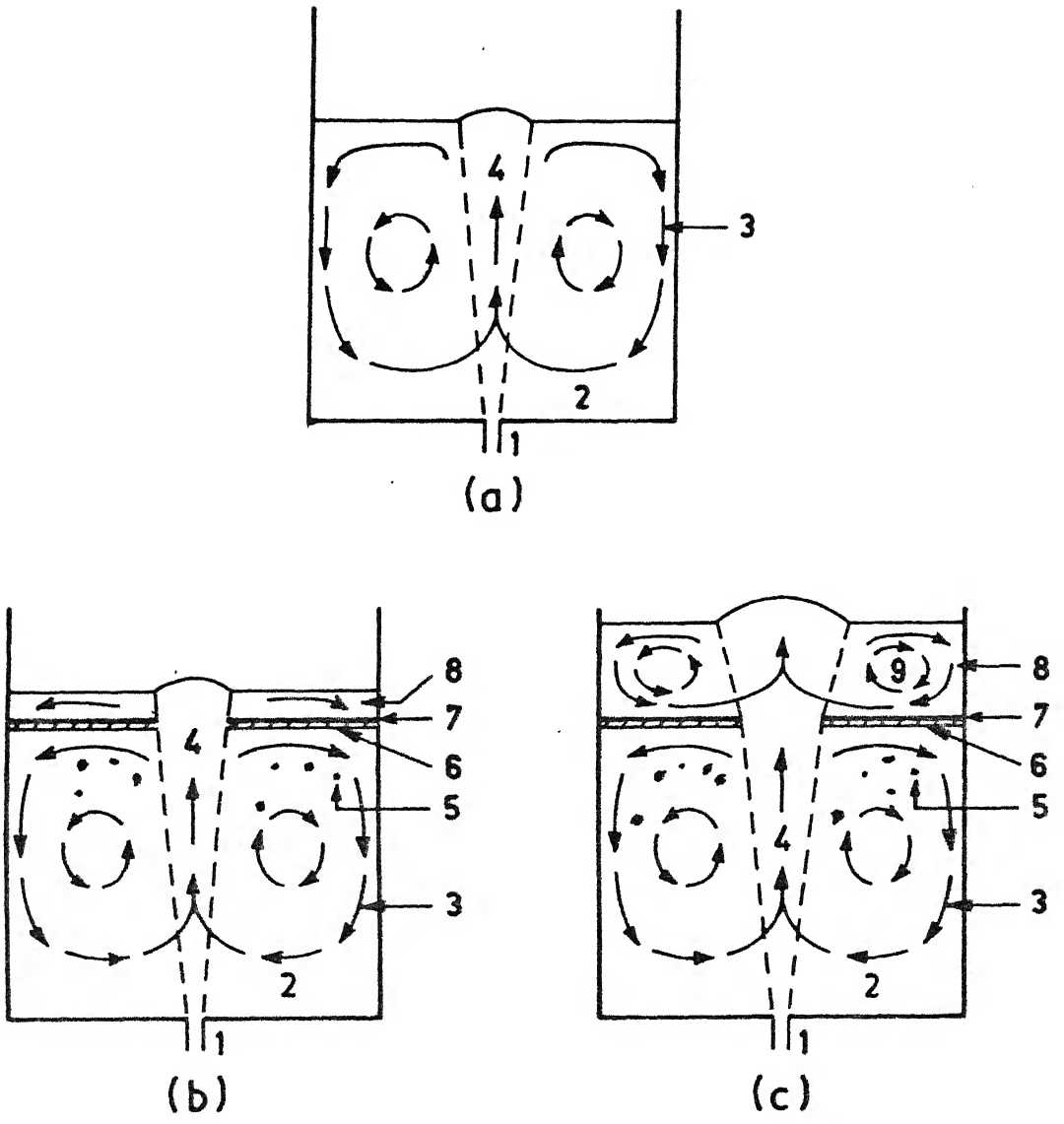

1. Nozzle 2. Phase-1 (dense) 3. Liquid circulation
4. Bubble plume 5. Entrained droplets (phase-2)
6. Zone of damped turbulence near interface
7. Interface (phase-1/phase-2) 8. Phase 2 (light)
9. Circulation in phase-2.

Fig. 4.23 : Schematic Representation of flow patterns in two immiscible liquids
a) single liquid, b) thin layer of phase 2,
c) thick layer of phase 2.

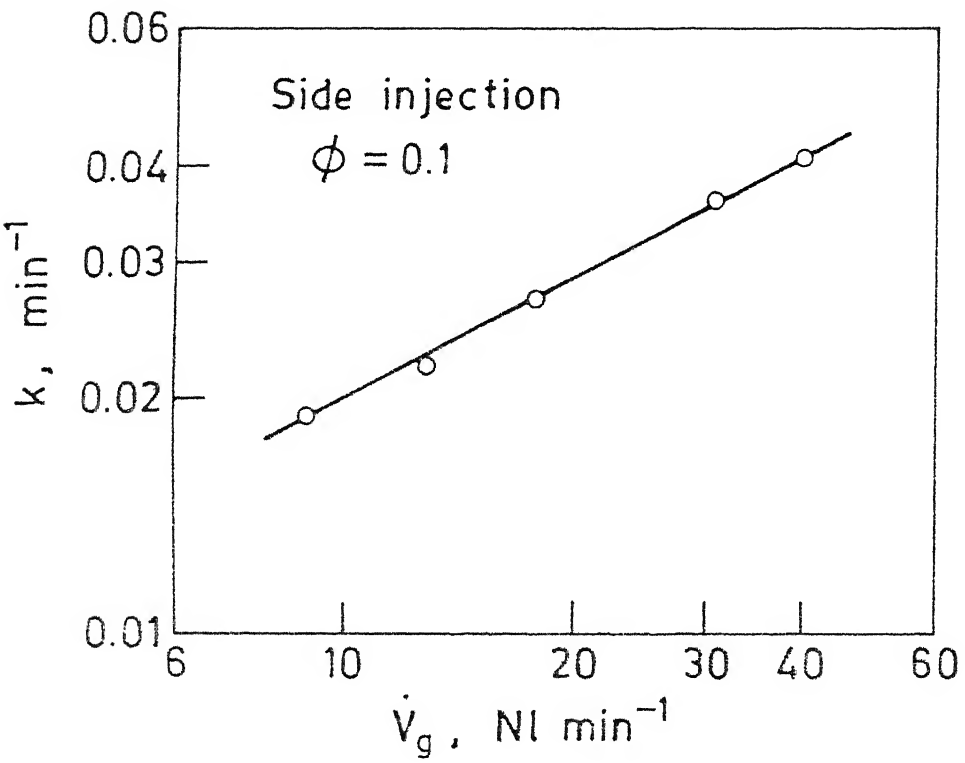

Fig. 4.24 : Variation of K as a function of gas flow rate for side injection.

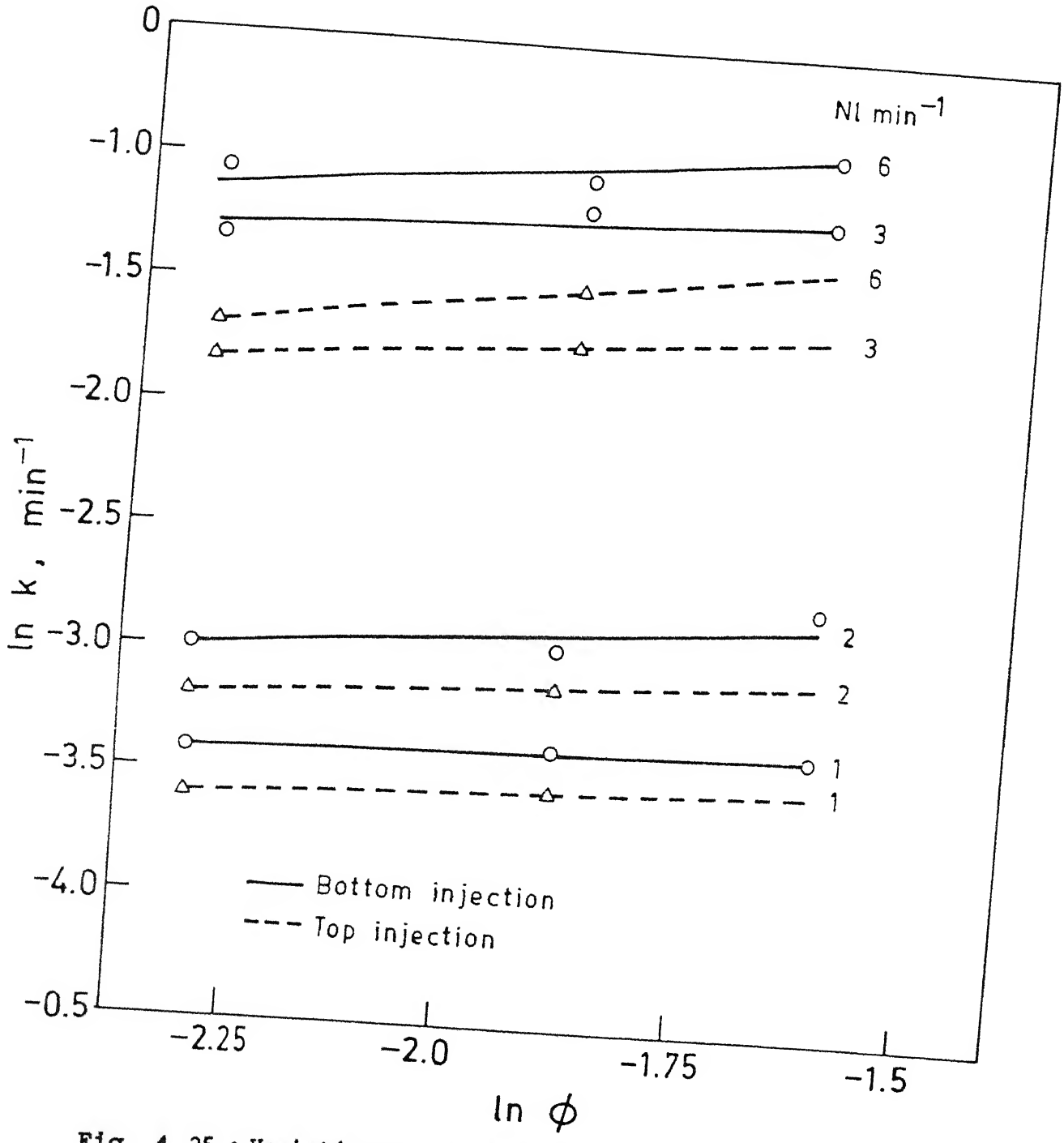

Fig. 4.25 : Variation of K as a function of volume fraction of slag for top and bottom injection.

Comparison of equations (4.3), (4.2) and (4.5). and (4.4) show that influence of volume fraction of slag has less effect in high gas flow region than low gas flow region (see exponent of ϕ in respective equation). For high gas flow rate oil droplet size stabilize because of coalescence of droplets so interfacial area does not change much with increase in volume fraction of slag.

4.8 COMPARISON OF TOP AND BOTTOM INJECTION

Figure 4.26 shows the variation of K with change of gas flow rate for top and bottom injection for $\phi = 0.1$ and Fig. 4.27 for $\phi = 0.15$.

It can be observed that as gas flow rate increases K increases and for bottom injection K is always higher than top injection, the relation between K and $\dot{v}_g$ for regime II is given in by equations (4.2) and (4.4) for bottom and top respectively. By these equation

$$\frac{K_b}{K_t} = 1.52\ \dot{v}_g^{0.072}\ \phi^{0.1276} \qquad (4.17)$$

The ratio K_b/K_t lies in the range 1.08 to 1.30 for regime III, equations (4.3) and (4.5) is used to draw the line for bottom and top respectively. By these two equation

$$\frac{K_b}{K_t} = 1.244\ \dot{v}_g^{-0.0998}\ \phi^{-0.01} \qquad (4.18)$$

In this range K_b/K_t is almost independent of either $\dot{v}_g$ or ϕ. Thus the ratio K_b/K_t is taken to 1.244.

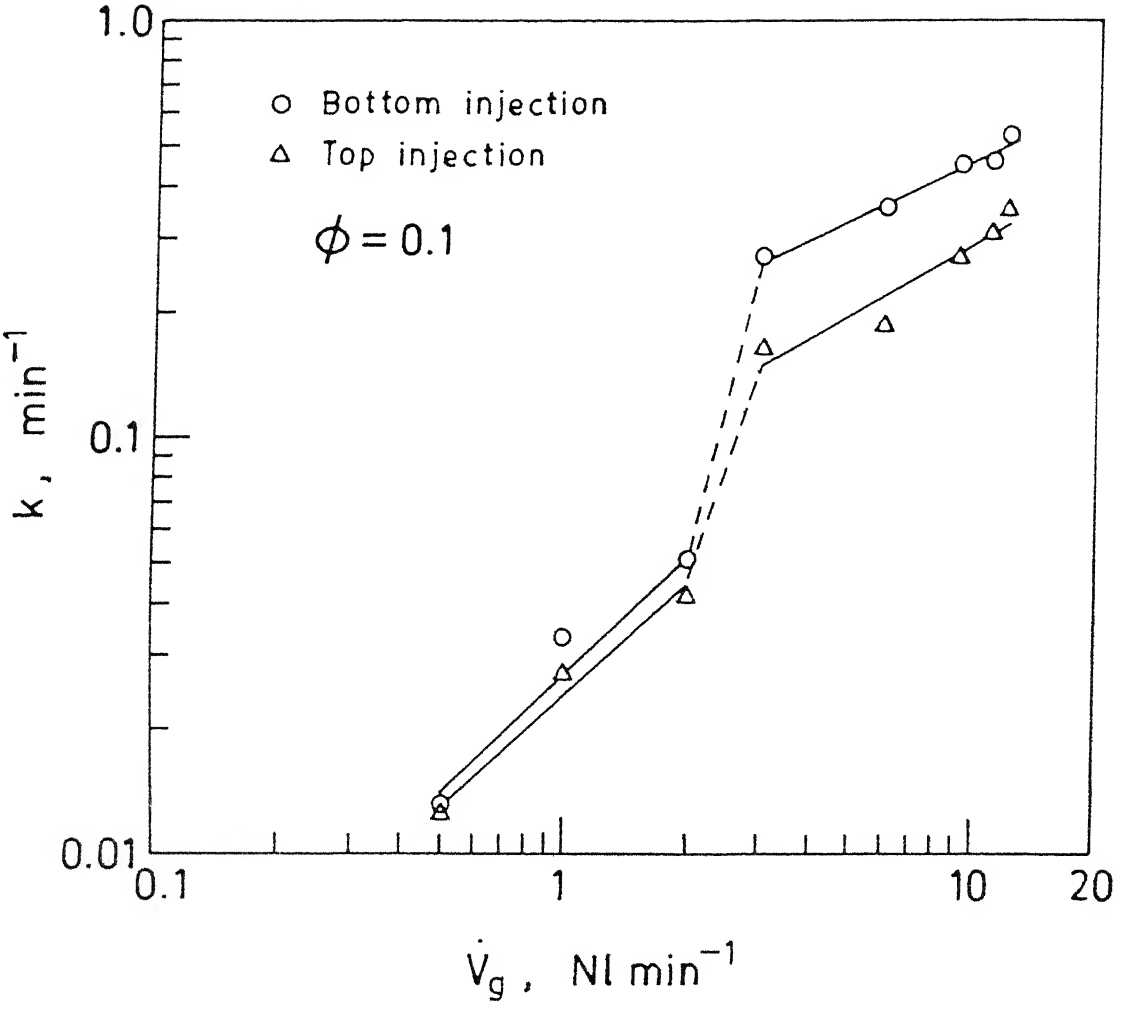

Fig. 4.26: Effect of bottom and top injection gas flow rate on rate constant for ϕ = 0.1.

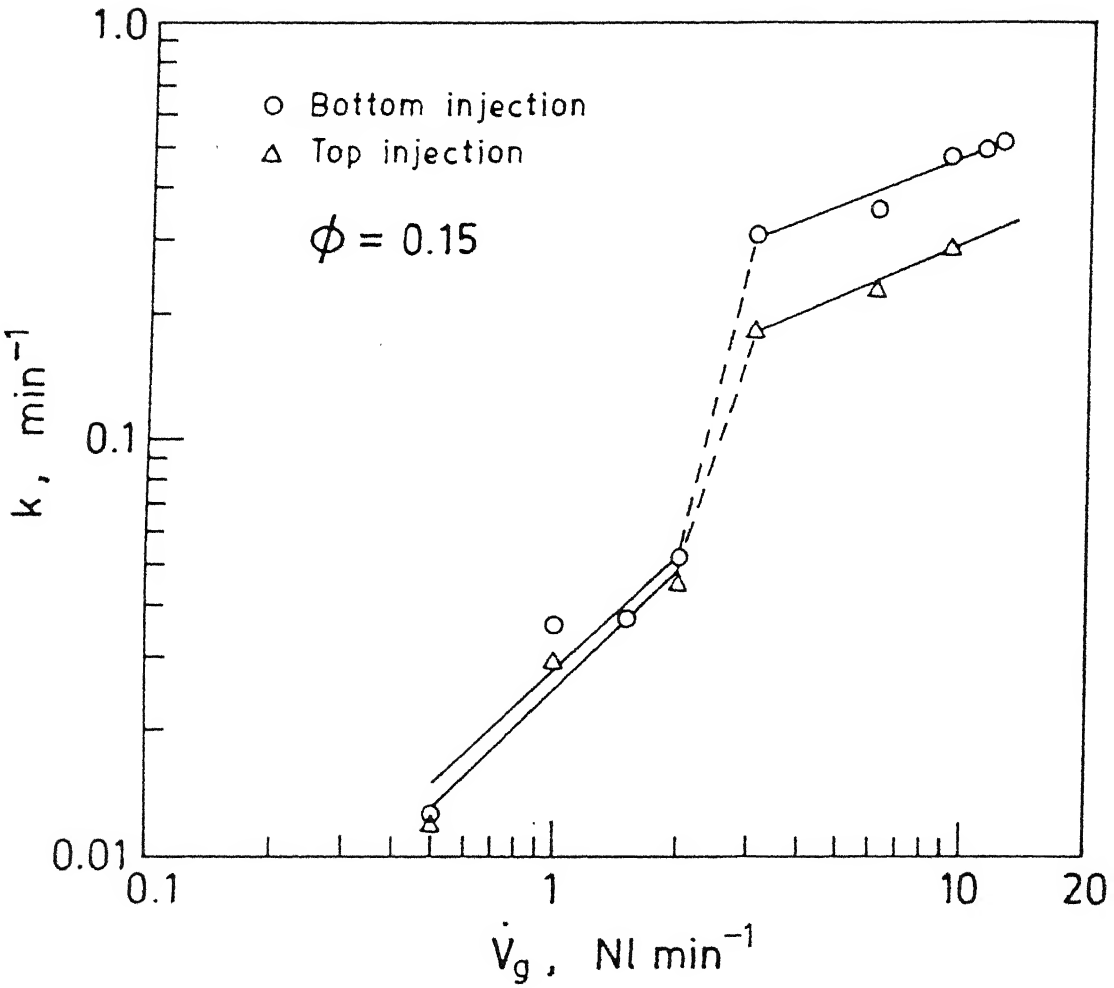

Fig. 4.27 : Effect of bottom and top injection on rate constant for ϕ = 0.15.

Considering that the metal side mass transfer rate is directly proportions to the liquid velocity induced by gas injection, the ratio K_b/K_t must also be proportional to respective liquid recirculation velocities i.e. U_b/U_t. According to the equation (2.4)

$$\frac{U_b}{U_t} = \beta^{1/3} \qquad (4.19)$$

Putting the value of $\beta = 0.5$ in the equation (4.17) we obtain

$$\frac{U_b}{U_t} = 1.26$$

which is surpringly in agreement with the value of the rate K_b/K_t. It is seen in K_b/K_t for both the region exponential term is very less so both top and bottom curve is almost parallel.

It can also be seen in both figure that for low flow rate region, the difference of K between bottom and an top injection is less than for high gas flow rate.

In bottom injection K is high because bubble is ascending to high speed so it gives much turbulence at the interface.

While in top blowing bubble penetrate downward against water to some distance and comes to either zero or very less velocity while changing it path from downward to upward and then it goes upward at the velocity of Stoke's law which is very less than the bottom injection velocity. So in bottom injection mass transfer rate is higher than top injection.

4.9 DETERMINATION OF β_m

According to equation (1.8) β_m can be determined only when interfacial area is known exactly. In experiments with slag injection the diameter of the slag droplet could be determined visuably better than gas injection experiments.

The droplets diameter was more or less constant (althou some variation were observed) for slag injection on experiments than gas injection. Therefore it was thought that the experime on slag injection could be used to determine the mass transfer coefficient in the present investigation.

The calculated value of β_m is listed in Table 4.3 by equation (1.8). In this calculation different value of d (following the visual observation) are assumed (0.2 cm, 0.3 cm and 0.4 cm). The value of U is calculated from the value of rate constant reported in Table 4.3).

In literature on mass transfer between two immiscible phases various empirical correlations are available. All these correlations are of the following forms:

$$Sh = A\, Sc^m\, Re^n \qquad (4.20)$$

where A, m, n are constant.

In order to calculate Sh and hence β_m by equation (4.20) the Reynold number must be known. The Reynold number contain a velocity term. The droplet velocity is determined by

$$151.72 = \frac{U^2}{d}\left(\frac{0.24}{dU} + \frac{0.4}{\sqrt{dU}} + 0.4\right) \qquad (4.21)$$

where U in cm/sec, d in cm.

Using equation (4.21) the value of U for d = 0.2, 0.

and 0.4 cm are determined. Value of U for d = 0.2 is 5.5 cm/sec for d = 0.3, it is 8 cm/sec, for d = 0.4 cm, it is 9.53 cm/sec.

The following empirical relation

$$Sh = 0.33\ Re^{0.6}\ Sc^{1/3} \tag{4.22}$$

is used to calculate Sh. The value of β_m is determined by equation,

$$Sh = \frac{\beta_m \cdot d}{D} \tag{4.23}$$

Value β_m is determined by equations (4.23) and (1.8) are listed in Table 4.3.

The comparison shows that the value of β_m from the two approaches lies in the same order of magnitude. For one particular case the value of β_m agrees very well. All other value of β_m calculated by experimental values of K are greater than those calculated by empirical equation.

This is due to fact that the empirical equation does not contain the influence of other parameter (such as depth of slag injector submergence, value of slag) on the K.

4.10 ESTIMATION OF INTERFACIAL AREA

For the purposes of mass transfer between two immiscible liquids, a knowledge of interfacial area available, for mass transfer is the most important. Since it was not possible to determine this interfacial area experimentally for gas injection experiments. An attempt has been made in the following to estimate the area using the informations of slag injection experiments.

The interfacial area is given by

$$A = \frac{K \; V_w}{\beta_m} \tag{4.24}$$

In this expression β_m is unknown. The empirical equation (4.22) is found to calculate satisfactorily the value of β_m for slag injection experiments in this investigation (See Table 4.3). The empirical eq. (4.22) will be used to calculate β_m for gas injection experiments. Putting the value of Reynolds and Schmidt No. in the eq. (4.22), we get

$$\frac{\beta_m \; d}{D_f} = 0.33 \left(\frac{U \, d \, \rho_L}{\mu}\right)^{0.6} \left(\frac{\nu}{D_f}\right)^{1/3} \tag{4.25}$$

To calculate β_m for gas injection experiments for eq. (4.25), the drop diameter and its velocity must be known. Photographic investigations have indicated that a range of droplet size (1 to 6 mm see section 4.1) is produced during gas injection. Further droplets due to which the drop diameter changes further.

Assuming that the most probable slag droplet size is 0.2 cm (actually there will a range of droplet size), one can calculate β_m as a function of U from the expression (4.25). Inserting the values of d = 0.2 cm, $D_f = 0.8346 \times 10^{-5}$ cm^2/s, $\rho_L = 1$ g cm^{-3}, $\nu = 0.01$ cm^2/sec. in (4.25) we get,

$$\beta_m = 8.825 \times 10^{-4} \; U^{0.6}. \qquad (4.26)$$

In the equation (4.26) U is the droplet velocity. In the literature the relationship between plume velocity and gas injection rate is available (see eq. 4.21). Plume velocity must be larger than the droplet velocity. The calculation made by eq. (2.4) and (4.21) has shown that droplet velocity is approximately 0.25 times plume velocity. Making use of this observation we get

$$U = \frac{15.2}{4} \; \dot{V}_g^{1/3} \qquad (4.27)$$

By eqs. (4.26) and (4.27) we get

$$\beta_m = 1.966 \times 10^{-3} \; \dot{V}_g^{0.2} \qquad (4.28)$$

Putting $\phi = 0.1$ in the expression (4.12), we get

$$K(\text{min}) = 0.1678 \; \dot{V}_g^{0.4312} \qquad (4.29)$$

Dividing eq. (4.29) by 60, we get

$$K(\text{sec}) = \frac{0.1678}{60} \; \dot{V}_g^{0.4312} \qquad (4.30)$$

In (4.30), K is in (sec), $\dot{V}_g$ in NL/min. By (4.24), (4.28) and (4.30) and $V_w = 5500\ cm^3$ we get

$$A = 7823.84\ \dot{V}_g^{0.2312} \qquad (4.31)$$

The planar surface area is in the present investigation is 1256 cm^2. Between the value of $\dot{V}_g$ 3 NL/min and 12 NL/min the droplet formation takes place. By eq. (4.31), the interfacial area would be 10086 cm^2 to 13895 cm^2. Increase in surface area due to gas injection in the regime of droplet formation is 8 to 11 times the planar surface area. The increase in rate constant in the droplet regime is 10 times to that of no droplet formation.

CHAPTER 5

SUMMARY AND CONCLUSION

The rate controlling process in many metallurgical reactions in gas stirred ladle is mass transfer between metal and slag. From the experimental results it can be concluded that

(1) Increase in gas injection rate increases the rate of transfer reaction irrespective of way of injection of gas.

(2) Three regimes of two phase mass transfer are observed in gas stirring in bottom and top injection which are explained by the break-up of the oil into droplets Causing an increase of the interfacial area. It is anticipated that a similar behaviour occurs in slag metal system.

(3) For similar gas flow rate, rate constant is more in bottom injector than top injection.

(4) No entrainment of oil droplet is found in side injection.

(5) Increase in volume fraction of oil from 0.1 to 0.2 increases rate constant by 20 percent.

SUGGESTION FOR FURTHER WORK

Further work can be done along the following lines:

1. Influence of different depth of submergence of lance on the mass transfer reaction between slag and metal phase.

2. Influence of initial concentration of the transferring entity on the mass exchange reaction.

3. Influence of different combination of nozzle on the mass transfer reaction between slag and metal phase.

REFERENCES

1. Ladle Metallurgy Principles and Practices by R.J. Fruehan.

2. Shigeo Asai, Masayuki Kawachi and Iwao Much paper.

3. Qu Ying, Lang Yun, Liu Ltu: Proceeding International Conference on Injection Metallurgy, Luka, Sweden, June 15-17, 1983, p. 21 : 1-21 : 16.

4. Jun-Ichi Sakare et al. : Trans. ISI Japan, Vol. 24, 1984, page B/204.

5. Simulation of Mixing Condition in Steelmaking, M.Tech. Thesis of Sohini Pal, Jan. 1989.

6. Seon-Hyo Kim and R.J. Fruehan, Met. Trans. 18B, 1987, pp. 381-390.

7. Masahiro et al., Trans. IS&J, Vol. 27, 1987, pp. 283-290.

8. K. Ogawa, ISIJ International, Vol. 29 (1989), No. 2, pp. 148-153.

9. Satish C. Koria and Chu Duc Khai, Trans. of IIM, Vol. 41, No. 2, April 1987, pp. 187-195.

10. K.W. Lanje, International Material Review, Vol. 33, No. 2, (1988), p. 53.

11. S.C. Koria, Consolidation of Approaches for Bubbling-jetting Transition of Gas Jets in Liquid, to be published in Ironmaking and Steelmaking.

12. Satish C. Koria, Steel Research 59 (1988), No. 11.

13. Kohtani, T. et al., Proc. 65th Steelmaking Conf. AIME, 1982, 211/20.

14. Nakanishi, et al., Proc. 65th Steelmaking Conf. AIME, 1982, 85/95.

15. Suzuki, K. - I. et al., Trans. Iron Steel Inst. Japan, 22 (1982), B-236.

16. Tanaka, S., Miyawaki, Y., Fachber. Huttenpraxis MWV 20 (1982), 786/95.

17. Gruner, H. et al., Stahlu. Eisen 104 (1984) 527/532.

18. Koria, S.C., Lange, K.W., Proc. 6th Japan, Germany Seminar, Tokyo, 1987, 91/107.

19. J. Szekely and N. El. Kadoah Ladle Metallurgy, Principles and Practices by R.J. Fruehan, p.

Table 4.1 : Change of concentration in aqueous phase with the change of slag percentage and gas flow rate in one hole bottom blown converter.

Vol. of aqueous phase = 5.5 litre

Vol. of aqueous phase use for titration = 25 ml

Initial concentration of benzoic acid in 2.32 gm/lit.

1 ml of KOH = 0.0025 gm of benzoic acid

4.1.1 Bottom Injection

Experimental conditions	Time (min)	Vol. of KOH used (ml)	Wt. of acid per litre bath (gm)	C_t/C_o
1	2	3	4	5
$\dot{V}_g$=0.5 NL/min	0	23.2	2.32	1.0
	5	22.7	2.27	0.98
ϕ = 0.1	10	22.6	2.26	0.97
	15	21.6	2.16	0.93
	20	21.5	2.15	0.925
	25	21.2	2.12	0.91
	30	20.8	2.08	0.90
$\dot{V}_g$=1 NL/min	0	23.2	2.32	1.0
	3	21.97	2.197	0.947
ϕ = 0.1	5	21.7	2.17	0.935
	10	21.0	2.10	0.906
	15	20.0	2.00	0.866
	20	19.7	1.97	0.849
	25	18.1	1.81	0.814
$\dot{V}_g$ = 2 NL/min	0	23.2	2.32	1.0
	2	21.8	2.18	0.939
ϕ = 0.1	5	21.8	2.18	0.938
	10	21.0	2.10	0.903
	15	19.2	1.92	0.83
	20	17.8	1.78	0.768
	25	17.3	1.73	0.745

1	2	3	4	5
$\dot{V}_g$ = 2.5 NL/min	0	34.0	2.32	1.0
	1	33.0	2.21	0.953
ϕ = 0.1	3	30.2	2.023	0.872
	5	28.8	1.929	0.831
	10	25.2	1.688	0.728
	15	23.4	1.567	0.675
	20	23.2	1.554	0.67
$\dot{V}_g$ = 3 NL/min	0	23.2	2.32	1.0
	1	21.6	2.16	0.929
ϕ = 0.1	3	18.7	1.87	0.808
	5	17.7	1.77	0.762
	10	15.7	1.57	0.675
	15	15.54	1.554	0.67
	20	15.54	1.554	0.67
$\dot{V}_g$ = 6.2 NL/min	0	23.2	2.32	1.0
	1	21.3	2.13	0.918
ϕ = 0.1	3	18.07	1.807	0.779
	5	16.88	1.688	0.727
	10	15.54	1.554	0.67
	15	15.54	1.554	0.67
$\dot{V}_g$ = 9 NL/min	0	23.2	2.32	1.0
	1	21.19	2.119	0.91
ϕ = 0.1	3	17.55	1.755	0.756
	5	16.34	1.634	0.704
	10	15.54	1.554	0.67
	15	15.54	1.554	0.67
$\dot{V}_g$ = 1 NL/min	0	23.2	2.32	1.0
	1	20.8	2.08	0.9
ϕ = 0.1	3	17.6	1.76	0.76
	5	15.54	1.554	0.67
	10	15.54	1.554	0.67
	15	15.54	1.554	0.67

1	2	3	4	5
$\dot{V}_g$ = 12 NL/min	0	23.2	2.32	1.0
ϕ = 0.1	1	21.2	2.12	0.91
	3	17.2	1.72	0.74
	5	15.54	1.554	0.67
	10	15.54	1.554	0.67
	15	15.54	1.554	0.67
$\dot{V}_g$ = 1 NL/min	0	23.2	2.32	1.0
ϕ = 0.1	1	22.1	2.21	0.95
	3	21.7	2.17	0.94
	5	20.9	2.09	0.9
	10	20.5	2.05	0.88
	15	19.3	1.93	0.85
	20	18.8	1.88	0.82
$\dot{V}_g$ = 2 NL/min	0	23.4	2.34	1.0
ϕ = 0.15	1	22.3	2.23	0.95
	3	21.5	2.15	0.92
	5	20.6	2.06	0.88
	10	19.3	1.93	0.78
	15	18.2	1.82	0.75
	20	17.5	1.75	0.748
$\dot{V}_g$ = 2.5 NL/min	0	57.8	2.34	1.0
ϕ = 0.15	1	55.0	2.24	0.96
	3	52.0	2.11	0.9
	5	49.0	1.99	0.85
	10	44.0	1.79	0.77
	15	40.6	1.65	0.71
	20	39.0	1.58	0.675
	30	36.8	1.50	0.64
$\dot{V}_g$ = 3 NL/min	0	23.4	2.34	1.0
ϕ = 0.15	1	21.3	2.13	0.91
	3	18.3	1.83	0.78
	5	16.4	1.64	0.7
	10	14.3	1.43	0.61
	15	13.8	1.38	0.59
	20	13.8	1.38	0.59

1	2	3	4	5
$\dot{V}_g$ = 6.2 NL/min	0	23.2	2.32	1.0
	1	21.1	2.11	0.91
ϕ = 0.15	3	17.1	1.71	0.74
	5	15.4	1.54	066
	10	14.1	1.41	0.61
	15	13.8	1.38	0.59
	20	13.8	1.38	0.59
$\dot{V}_g$ = 9 NL/min	0	23.4	2.34	1.0
ϕ = 0.15	1	22.8	2.28	0.898
	3	16.4	1.64	0.7
	5	14.7	1.47	0.63
	10	13.8	1.38	0.59
	15	13.8	1.38	0.59
	20	13.8	1.38	0.59
$\dot{V}_g$ = 11 NL/min	0	23.2	2.32	1.0
	1	21.1	2.11	0.9
ϕ=0.15	3	15.78	1.578	0.68
	7	13.78	1.38	0.59
	10	13.78	1.38	0.59
$\dot{V}_g$ = 12 NL/min	0	23.2	2.32	1.0
	1	20.8	2.08	0.9
ϕ = 0.15	3	15.6	1.56	0.67
	5	13.8	1.38	0.59
	7	13.8	1.38	0.59
	10	13.8	1.38	0.59
	15	13.8	1.38	0.59
$\dot{V}_g$ = 1 NL/min	0	23.2	2.32	1.0
	1	23.1	2.31	0.996
ϕ = 0.20	3	21.5	2.15	0.93
	5	21.1	2.11	0.91
	10	19.8	1.98	0.85
	15	18.8	1.88	0.81
	20	18.1	1.81	0.78
	31	16.2	1.62	0.70
	46	15.5	1.55	0.67

1	2	3	4	5
$\dot{V}_g$ = 2 NL/min	0	23.2	2.32	1.0
	1	22.4	2.24	0.97
ϕ = 0.2	3	20.9	2.09	0.9
	5	19.9	1.99	0.86
	10	18.0	1.8	0.78
	15	16.8	1.68	0.73
	20	15.5	1.55	0.67
	30	14.5	1.45	0.63
	45	13.1	1.31	0.565
$\dot{V}_g$ = 3 NL/min	0	23.2	2.32	1.0
ϕ^g = 0.2	1	21.4	2.14	0.92
	3	17.2	1.72	0.74
	5	15.2	1.52	0.66
	10	13.0	1.30	0.56
	15	12.6	1.26	0.54
	20	12.6	1.26	0.54
	30	12.6	1.26	0.54
$\dot{V}_g$ = 6.2 NL/min	0	23.2	2.32	1.0
ϕ = 0.2	1	20.4	2.04	0.88
	3	15.2	1.52	0.65
	5	13.9	1.39	0.60
	10	12.6	1.26	0.54
	15	12.6	1.26	0.54
$\dot{V}_g$ = 9 NL/min	0	23.2	2.32	1.0
ϕ = 0.2	1	20.0	2.0	0.86
	3	15.0	1.5	0.65
	5	13.4	1.34	0.58
	10	12.6	1.26	0.54
	15	12.6	1.26	0.54

4.1.2 : Top Injection of Gas

Depth of Submergence of Lance = 0.5

1	2	3	4	5	
V_g=0.5 NL/min	0	23.2	2.32	1.0	
	5	22.86	2.286	0.986	
ϕ = 0.1	10	22.18	2.218	0.956	
	15	21.95	2.195	0.946	
	20	21.5	2.15	0.927	
	25	21.0	2.1	0.907	
Slag = 10%	0	23.2	2.32	1.0	1.0
V_g = 1 NL/min	5	22.2	2.22	0.957	0.867
	10	21.2	2.12	0.914	0.733
	15	20.6	2.06	0.89	0.653
	20	20.14	2.014	0.868	0.592
	25	19.37	1.937	0.84	0.50
Slag = 10%	0	23.2	2.32	1.0	1.0
V_g = 2 NL/min	5	21.6	2.16	0.93	0.787
	10	20.5	2.05	0.88	0.64
	15	19.8	1.98	0.85	0.547
	20	19.0	1.90	0.82	0.44
	25	18.22	1.822	0.785	0.336
Slag = 19%	0	41	2.36	1.0	
$\dot{V}_g$ = 2.5 NL/min	1	39.4	2.229	0.961	
	3	38.2	2.16	0.93	
	5	37.4	2.12	0.914	
	10	34.6	1.96	0.845	
	15	32.8	1.856	0.8	
	20	31.0	1.754	0.756	

1	2	3	4	5
Slag = 10%	0	23.2	2.32	1.0
$\dot{V}_g$ = 3 NL/min	1	21.7	2.17	0.935
	3	20.6	2.06	0.888
	5	19.35	1.935	0.834
	10	17.1	1.71	0.74
	15	15.7	1.57	0.677
Slag = 10%	0	23.2	2.32	1.0
$\dot{V}_g$ = 6 NL/min	1	21.5	2.15	0.93
	3	20.27	2.027	0.874
	5	19.24	1.924	0.829
	10	16.75	1.675	0.722
	15	15.7	1.67	0.677
Slag = 10%	0	23.2	2.32	1.0
$\dot{V}_g$ = 9 NL/min	1	21.4	2.14	0.922
	3	19.1	1.91	0.823
	5	17.43	1.743	0.75
	10	16.2	1.62	0.698
	15	15.84	1.584	0.680
$\dot{V}_g$ = 11 NL/min	0	23.2	2.32	1.0
ϕ = 0.10	1	21.6	2.16	0.93
	3	18.9	1.89	0.815
	5	17.4	1.74	0.75
	10	15.7	1.57	0.677
	15	15.7	1.57	0.677
Slag = 10%	0	23.2	2.32	1.0 1.0
$\dot{V}_g$ = 12 NL/min	1	21.6	2.16	0.93 0.787
	3	18.8	1.88	0.81 0.41
	5	17.2	1.72	0.74 0.2
	10	15.9	1.59	0.68 0.027
	15	15.7	1.57	0.676 0

1	2	3	4	5	6
$\dot{V}_g$=0.5NL/min	0	23.2	2.32	1.0	1.0
ϕ = 0.15	5	22.75	2.275	0.98	0.952
	10	22.0	2.2	0.95	0.87
	15	21.7	2.17	0.935	0.838
	20	21.2	2.12	0.914	0.785
	25	20.64	2.064	0.89	0.722
$\dot{V}_g$=1 NL/min	0	23.2	2.32	1.0	1.0
	5	21.8	2.18	0.94	0.848
ϕ =0.15	10	20.9	2.09	0.9	0.75
	15	19.9	1.99	0.86	0.64
	20	19.1	1.91	0.82	0.554
	25	18.6	1.86	0.80	0.5
$\dot{V}_g$=2 NL/min	0	23.2	2.32	1.0	1.0
	5	21.1	2.11	0.41	0.77
ϕ=0.15	10	19.7	1.97	0.85	0.62
	15	18.7	1.87	0.805	0.51
	20	17.9	1.79	0.77	0.42
	25	17.0	1.70	0.73	0.33
$\dot{V}_g$=3 NL/min	0	23.2	2.32	1.0	1.0
	1	21.5	2.15	0.927	0.815
	3	19.1	1.91	0.823	0.609
	5	18.0	1.8	0.776	0.378
	10	15.56	1.556	0.67	0.17
	15	14.0	1.40	0.603	-
	20	14.0	1.40	0.603	-

1	2	3	4	5	6
$\dot{V}_g$=6 NL/min	0	23.2	2.32	1.0	1.0
	1	20.5	2.05	0.884	0.706
ϕ = 0.15	3	18.2	1.82	0.784	0.456
	5	16.8	1.68	0.724	0.304
	10	15.1	1.51	0.65	0.109
	15	14.0	1.40	0.603	0
	20	14.0	1.40	0.603	0
$\dot{V}_g$=9 NL/min	0	23.2	2.32	1.0	1.0
	1	20.0	2.0	0.862	0.652
	3	17.4	1.74	0.75	0.369
ϕ = 0.15	5	15.7	1.57	0.677	0.185
	10	14.6	1.46	0.629	0.065
	15	14.0	1.40	0.603	0
	20	14.0	1.40	0.603	0

Table 4.1.3. : Side Injection
Volume of Aqueous/Phase = 12 litre
Volume fraction of slag = 0.1

1	2	3	4	5
V_g=9NL/min	0	23.2	2.32	1.0
ϕ = 0.1	1	23.1	2.31	0.987
	3	22.79	2.279	0.946
	5	22.68	2.268	0.932
	10	21.81	2.182	0.819
	15	21.04	2.114	0.731
	20	20.62	2.062	0.663
	25	20.3	2.030	0.597
	30	20.0	2.000	0.582
	35	19.75	1.975	0.55
	40	19.54	1.954	0.522
	45	19.38	1.938	0.501

1	2	3	4	5
$\dot{V}_g$=13NL/min	0	23.2	2.32	1.0
	1	22.79	2.279	0.982
	3	22.65	2.265	0.976
	5	22.14	2.214	0.954
	10	21.59	2.159	0.931
	15	20.93	2.093	0.902
	20	20.44	2.044	0.885
	25	19.98	1.998	0.865
	30	19.50	1.95	0.84
	35	19.37	1.937	0.835
	40	19.20	1.97	0.83
	45	19.10	1.91	0.82

1	2	3	4	5
$\dot{V}_g$=18NL/min	0	23.2	2.32	1.0
	1	22.5	2.25	0.97
	3	22.3	2.23	0.961
	5	21.81	2.181	0.94
	10	21.21	2.121	0.914
	15	20.71	2.071	0.893
	20	20.01	2.001	0.862
	25	19.52	1.952	0.84
	30	18.91	1.891	0.815
	35	18.76	1.876	0.81
	40	18.60	1.86	0.80
	45	18.45	1.845	0.794

1	2	3	4	5
$\dot{V}_g$=30NL/min	0	23.2	2.32	1.0
	1	21.97	2.191	0.944
	3	21.81	2.181	0.94
	5	21.31	2.131	0.918
	10	20.66	2.066	0.89
	15	19.86	1.986	0.856
	20	19.37	1.937	0.83
	25	18.6	1.86	0.80
	30	18.22	1.822	0.785
	35	18.10	1.81	0.78
	40	17.80	1.78	0.77
	45	17.60	1.76	0.76

1	2	3	4	5
$\dot{V}_g$=40NL/min	0	23.2	2.32	1.0
	1	21.8	2.18	0.94
	3	21.3	2.13	0.918
	5	21.05	2.105	0.91
	10	20.65	2.065	0.89
	15	19.50	1.95	0.841
	20	19.0	1.9	0.819
	25	18.22	1.822	0.785
	30	17.80	1.78	0.77
	35	17.70	1.77	0.76
	40	17.50	1.75	0.75
	45	17.3	1.73	0.745

Table 4.2 : Rate Constant as a Different Parameter of Injection

Experimental Conditions	$\dot{V}$ (NL/min)	K(min^{-1})
Bottom Injection ϕ = 0.1	0.5	0.013
	1.0	0.033
	1.5	0.0353
	2.0	0.05
	2.5	0.167
	3.0	0.265
	6.2	0.35
	9.0	0.447
	11.0	0.454
	12.0	0.531
Bottom Injection ϕ = 1.5	0.5	0.0136
	1.0	0.0343
	2.0	0.052
	2.5	0.084
	3.0	0.31
	6.2	0.3505
	9.0	0.479
	11.0	0.5
	12.0	0.532
Bottom Injection	1	0.0349
	2	0.064
	3	0.312
	6.2	0.41
	9.0	0.49

Table 4.2 (Continued):

Experimental Conditions	$\dot{V}g$ (NL/min)	K(min^{-1})
Top Injection ϕ = 0.1	0.5	0.0122
	1.0	0.0276
	2.0	0.0715
	2.5	0.0678
	3.0	0.162
	6.2	0.186
	9.0	0.274
	11.0	0.314
	12.0	0.349
Top Injection ϕ = 0.1	0.5	0.0126
	1.0	0.0288
	2.0	0.448
	3.0	0.18
	6.2	0.228
	9.0	0.29
Side Injection ϕ = 0.10	9	0.0191
	13	0.0222
	18	0.0271
	30	0.0362
	40	0.0413

Table 4.3 :

d_n (mm)	ϕ	β_i	$K(sec^{-1})$	β_m (cm/sec) d = 0.2 cm	d = 0.3 cm	d = 0.4 cm
2	0.1	0.5	1.366×10^{-3}	4.55×10^{-4}	6.83×10^{-4}	9.1×10^{-4}
2	0.1	0.95	1.662×10^{-3}	5.54×10^{-4}	8.31×10^{-4}	1.108×10^{-3}
1	0.1	0.5	4.305×10^{-3}	1.435×10^{-3}	2.15×10^{-3}	2.87×10^{-3}
1	0.1	0.95	5.929×10^{-3}	1.976×10^{-3}	2.96×10^{-3}	3.95×10^{-3}
1	0.05	0.5	2.668×10^{-3}	1.78×10^{-3}	2.67×10^{-3}	3.56×10^{-3}
1	0.05	0.95	3.346×10^{-3}	2.23×10^{-3}	3.346×10^{-3}	4.46×10^{-3}
BY EXPERIMENTAL FORMULA				2.45×10^{-3}	2.612×10^{-3}	2.586×10^{-3}

Tabl4 4.4 : Injection of Slag

Experimental condition	Time, sec	Vol. of KOH used (ml)	Wt. of acid per litre (C_t)	C_t/C_o
1	2	3	4	5
ϕ = 0.1	0	23.2	2.32	1.0
d_n = 1 mm	30	21.47	2.147	0.925
B_1 = 0.5	60	20.91	2.071	0.901
	90	20.63	2.063	0.889
	120	20.08	2.008	0.865
	150	19.52	1.952	0.841
	180	19.07	1.907	0.822
	210	18.85	1.885	0.8125
1	2	3	4	5
ϕ = 0.1	0	23.2	2.32	1.0
d_n = 1 mm	30	21.08	2.108	0.909
B_1 = 0.95	60	20.58	2.058	0.887
	90	19.58	1.958	0.844
	120	18.96	1.896	0.817
	150	18.57	1.857	0.8
	180	18.35	1.835	0.791
	210	18.01	1.801	0.776

Table 4.4 (Continued):

1	2	3	4	5
ϕ = 0.1	0	23.2	2.32	1.0
	30	22.64	2.264	0.976
	60	22.47	2.247	0.969
	90	22.30	2.23	0.961
	120	22.14	2.214	0.954
	150	21.8	2.18	0.94

1	2	3	4	5
ϕ = 0.1	0	23.2	2.32	1.0
B_1=0.95	30	22.42	2.242	0.966
d_n=2 mm	60	22.25	2.225	0.959
	90	22.03	2.203	0.9495
	120	21.92	2.192	0.945
	150	21.64	2.164	0.933

1	2	3	4	5
ϕ = 0.05	0	23.2	2.32	1.0
B_1=0.95	30	22.53	2.253	0.971
d_n=2 mm	60	22.36	2.236	0.964
	90	22.2	2.22	0.957

Table 4.4 (Continued):

1	2	3	4	5
ϕ = 0.05	0	23.2	2.32	1.0
B_1=0.95	30	22.7	2.27	0.978
d_n = 2 mm	60	22.53	2.253	0.971
	90	22.36	2.236	0.964

APPENDIX 1

CALCULATION OF MODEL PARAMETERS

Froud number has been calculated by two ways one is based on superficial gas injection velocity and the other based on the plume velocity.

Froud No. based on superficial gas injection velocity is given by

$$N_{Fr} = \frac{\rho_g \, u^2}{\rho_L \, g \, H} \qquad (1)$$

$$u = \frac{4 \, \dot{V}_g}{\pi \, d_n^2 \, N} \qquad (2)$$

Combining equations (1) and (2) and rearranging, we get

$$N_{Fr} = 0.811 \; \frac{\rho_g}{\rho_L} \; \frac{\dot{V}_g^2}{N^2 \, d_n^4 \, Hg} \qquad (3)$$

Since N = 1.

$$N_{Fr} = \frac{0.082 \, \dot{V}_g^2}{\rho_L \, d_n^4 \cdot H} \qquad (4)$$

Now by taking $\rho_1 = 1.32$ kg/m^3, H = 0.18 m, d_n = 1 mm, ρ = 1000 kg/m^3.

$$N_{Fr} = 6.01 \times 10^8 \cdot \dot{V}_g^2$$

where $\dot{V}_g$ = Nm^3/sec.

$$N_{Fr} = 0.167 \, \dot{V}_g^2, \; \dot{V}_g = \text{NL/min.}$$

Energy is calculated by the following equation:

$$\dot{\varepsilon} = \frac{6.18\ \dot{V}_g\ T_L}{V_w}\left[\ \ln\left(1 + \frac{\rho_L\ gH}{Pr}\right) + \left(1 - \frac{T_g}{T_L}\right)\ \right] \qquad (10)$$

Now by using,

$T_L = 298^{\circ}K$

$T_g = 298^{\circ}K$

$\rho_L = 1000\ kg/m^3$

$H = 0.18\ m$

$g = 9.81\ m/sec^2$

$P_2 = 1.013 \times 10^5\ kg\ m^{-1}\ sec^{-2}$

$V_w = 5.5 \times 10^{-3} m^3$

$$\dot{\varepsilon} = 5786.5\ V_g \qquad (11)$$

V_g in Nm^3/min

So $\dot{\varepsilon} = 5.786\ \dot{V}_g$ where $\dot{V}_g$ in NL/min.

Froud No. based on plume velocity

$$N'_{Fr} = \frac{U_P^2}{g \times 0.37 \times H}$$

$$U_P = K. \frac{\beta^{1/3} \times H^{1/4} \times \dot{V}_g^{1/3}}{R^{1/3}} \quad (5)$$

Now by putting for bottom injection $\beta = 1$ and for top injection $\beta = 0.5$, $H = 0.18$ m, $R = 0.1$ m

$$K = 4.19$$

For bottom injection

$$U_P = 4.19 \times \frac{1 \times (0.18)^{1/4} \cdot \dot{V}_g^{1/3}}{(0.1)^{1/3}}$$

$$U_P = 5.96 \dot{V}_g^{1/3} \text{ m/sec. } \dot{V}_g \text{ in } Nm^3/sec \quad (6)$$

$$= 0.152 \dot{V}_g^{1/3} \cdot \dot{V}_g \text{ in NL/min.} \quad (7)$$

Now,

$$N'_{Fr} = \frac{(5.96 \dot{V}_g^{1/3})^2}{4.81 \times 0.37 \times 0.18}$$

$$= 54.37 \dot{V}_g^{2/3}$$

$$= 54.37 \times \left(\frac{\dot{V}_g \times 10^{-3}}{60}\right)^{2/3}$$

$$= 0.0345 (\dot{V}_g)^{2/3}$$

where $\dot{V}_g$ is in NL/min. (8)

U_P for top $= 0.12 \dot{V}_g^{1/3}$, V_g in NL/min. for bottom injection

$$N'_{Fr} = 0.0217 \dot{V}_g^{2/3} \quad (9)$$

V_g in NL/min.

$\dot{V}_g$	U_p for bottom m/sec	U_p for top m/sec	Energy watt/m^3	N_{Fr}	N'_{Fr} for bottom injection	N'_{Fr} for top injection
0.5	0.12	0.095	2.873	0.072	0.0217	0.017
1.0	0.152	0.12	5.786	0.167	0.0345	0.0217
2.0	0.19	0.15	11.572	0.67	0.054	0.034
3.0	0.217	0.17	17.358	1.5	0.072	0.045
6.2	0.239	0.19	35.87	6.4	0.088	0.055
9	0.317	0.25	52.07	13.52	0.149	0.094
12	0.348	0.276	69.43	24.04	0.181	0.114

APPENDIX II

CALCULATION OF INTERFACIAL AREA

$$Sh = 0.33\ Re^{0.6}\ (Sc)^{0.33} \tag{12}$$

$$Sc = \frac{\nu}{D_f} \tag{13}$$

$$D_f = 0.346 \times 10^{-5}\ cm^2/sec, V = 0.01\ gm^{-3}\ sec^{-1}$$

$$Sc = 1198.18$$

$$Sh = 0.33 \left(\frac{U\,d}{\mu}\right)^{0.6} \cdot (1198.18)^{0.33}$$

$$= 54.25\ U^{0.6}\ d^{0.6} \tag{14}$$

$$Sh = \frac{\beta_m \cdot d}{D_f} = 0 \tag{15}$$

$$\frac{\beta_m \cdot d}{0.8346 \times 10^{-5}} = 54.25\ U^{0.6}\ d^{0.6}$$

$$\beta_m = 4.528 \times 10^{-4}\ \frac{U^{0.6}}{10.4} \tag{16}$$

In the Eq. 5, U is the velocity of the droplet which is taking past in the mass transfer process. Droplet velocity is much smaller than the plume velocity. In the following, only bottom gas injection is considered. From equation (4.21) for d = 0.2 to 0.4, U = 5.5 to 9.5 from equation (7), U is 21.7 to 34.8 cm/sec so the equation for droplet velocity from equation (7)

$$U = 3.8\ V_g^{.1/3}\ /4 \tag{17}$$

so

$$\beta_m = 4.528 \times 10^{-4} \cdot \frac{(3.8\ \dot{V}_g^{1/3})^{0.6}}{d^{0.4}} \quad (18)$$

$$= 1.07 \times 10^{-3} \frac{\dot{V}^{0.2}}{d^{0.2}} \quad (19)$$

By equation (4.24)

$$A = \frac{K \cdot V_w}{\beta_m} \quad (20)$$

K is a rate constant and depends on $\dot{V}_g$ and ϕ. In the droplet formation regime the variation of K is given by

$$K(\text{sec}) = 0.2516\ (\dot{V}_g)^{0.4312}\ \phi^{0.176}/60 \quad (21)$$

$$V_w = 5500\ \text{cm}^3$$

$$A = \frac{0.2516(\dot{V}_g)^{0.4312}\ \phi^{0.1760} \times 5500}{60 \times 1.01 \times 10^{-3}\ \dot{V}_g^{0.2}/d^{0.4}} \quad (22)$$

$$A = 22863.74\ \dot{V}_g^{0.2312}\ \phi^{0.176}\ d^{0.4} \quad (23)$$

Here $\dot{V}_g$ in NL/min and d in cm in order to get A in cm^2.

Typical case $\phi = 0.1$, $d = 0.2$ cm

$$A = \dot{V}_g^{0.2312}$$

Planar surface area $= \pi D^2$ (24)

$(A_p) = 1256\ \text{cm}^2$.

At $\dot{V}_g$, 3 and 12 NL/min the value of A is calculated by equation (24) 10311.54 cm^2 and 14207.56 cm^2. The ratio between A/A_p is 8.2 and 11.31. If it is assumed that 550 ml volume of slag has been converted to 0.2 cm droplet dia, then the area available would have been 16500 cm^2.